

Synthetic efforts toward lagunamide C: route development and implementation upon a model system

by

Chelsea Hanks

B.S., Kansas Wesleyan University, 2013

A THESIS

Submitted in partial fulfillment of the requirements for the degree

MASTER OF SCIENCE

Department of Chemistry  
College of Art and Sciences

KANSAS STATE UNIVERSITY  
Manhattan, Kansas

2017

Approved by:

Major Professor  
Dr. Ryan J. Rafferty

# **Copyright**

© Chelsea Weese 2017.

## Abstract

The lagunamides are a group of natural products derived from cyanobacterium. Lagunamides A, B, and C have shown impressive cytotoxicity towards a panel of cancer and malarial cell lines. Each of the lagunamide family members share structural similarities within their polypeptide backbone, but the polyketide units with A/B differ from C by an additional methylene insertion. The total synthesis of lagunamide A and an analog of lagunamide B have been reported by Dai and Pal's groups, respectively. The synthesis of lagunamide A was completed first by Dai and proved that the original structural elucidation was incorrect. With this inaccurate stereochemical assignment, it was suspected that this inaccuracy also appeared in the structural elucidation of Lagunamide B that was completed by Pal. It is alleged that these inaccuracies have occurred in the stereochemical assignments of the isolated structure of lagunamide C.

In addition to the stereochemical inaccuracies, a new synthetic route is necessary to synthesize lagunamide C. The structures of lagunamides A and C are nearly identical, except for the addition of one carbon in the polyketide portion of lagunamide C. This additional carbon disallows the use of same synthetic methods applied on lagunamide A to be employed on the synthesis of the polyketide portion of lagunamide C.

This work will discuss a modular approach towards the synthesis of lagunamide C. Model systems were employed to test the validity and success of the proposed route. Key steps of the proposed synthetic route include a titanium mediated mixed aldol reaction, cyclopropanation, and Charette cyclopropane ring-opening. The current synthetic route is shown to be scalable and possessing optimizable transformations. These steps have proven to be successful with the model systems and have laid the groundwork for the synthesis of the target compound, lagunamide C.

# Table of Contents

List of Figures .....	vii
List of Tables .....	viii
List of Schemes .....	ix
Abbreviations .....	xi
Acknowledgements .....	xiii
Dedication .....	xiv
Chapter 1 - Introduction to Natural Products.....	1
1.0 Introduction.....	1
1.0.1 Botox .....	2
1.0.2 Aspirin.....	3
1.0.3 Taxol .....	4
1.1 Total synthesis .....	6
1.2 Natural products and cancer .....	8
1.3 Summary.....	11
Chapter 2: Previous Synthesis and Proposed Work.....	13
2.0 Previous synthetic work.....	13
2.0.1 Synthesis of lagunamide A .....	14
2.0.2 Synthesis of lagunamide B analog .....	18
2.1 Retrosynthetic analysis of lagunamide C.....	21
2.2 Proposed work of the polyketide fragment.....	23
2.2.1 Module I.....	23
2.2.2 Module II .....	25

2.2.3 Module III .....	25
2.3 Summary .....	26
Chapter 3: Current synthetic work .....	28
3.1 Introduction to the methyl-truncated analog of lagunamide C .....	28
3.2 Module I .....	29
3.3 Module II .....	33
3.4 Summary .....	36
Chapter 4: Conclusion and Future Work .....	37
4.1 Conclusion .....	37
4.2 Future Work .....	38
Chapter 5: Experimental Procedures .....	39
L-Valinol .....	39
(S)-4-isopropylthiazolidine-2-thione .....	41
(S)-1-(4-isopropyl-2-thioxothiazolidin-3-yl)ethan-1-one .....	42
(R)-3-hydroxy-1-((S)-4-isopropyl-2-thioxothiazolidin-3-yl)hexan-1-one .....	44
(R)-3-((tert-butyldimethylsilyl)oxy)-1-((S)-4-isopropyl-2-thioxothiazolidin-3-yl)hexanone ..	47
(R)-3-((tert-butyldimethylsilyl)oxy)hexanol .....	49
(R)-3-((tert-butyldimethylsilyl)oxy)hexanal .....	51
Methyl (R,E)-5-((tert-butyldimethylsilyl)oxy)oct-2-enoate .....	52
(R,E)-5-((tert-butyldimethylsilyl)oxy)oct-2-en-1-ol .....	55
(2-((R)-2-((tert-butyldimethylsilyl)oxy)pentyl)cyclopropyl)methanol .....	57
Tert-butyl(((2R)-1-(2-(iodomethyl)cyclopropyl)pentan-2-yl)oxy)dimethylsilane .....	59
Tert-butyldimethyl(((4R)-6-methyloct-7-en-4-yl)oxy)silane .....	62

Chapter 6: Bibliography..... 64

## List of Figures

<b>Figure 1</b> Quarternary Structure of Botulinum Toxin A .....	2
<b>Figure 2</b> Structure of Taxol.....	5
<b>Figure 3</b> Cancer-fighting natural products derived from marine organisms.....	9
<b>Figure 4</b> Structures and IC <sub>50</sub> values of select aurilides and lagunamides .....	10
<b>Figure 5</b> Polyketide fragments of lagunamides A, B, and C.....	13
<b>Figure 6</b> Published and revised structures of lagunamide A.....	14
<b>Figure 7</b> Lagunamide B and analog of lagunamide B .....	18
<b>Figure 8</b> Diastereomers of lagunamide C polyketide.....	21
<b>Figure 9</b> Compound synthesized by Zhou Group vs. Compound <b>73</b> .....	31
<b>Figure 10</b> Proton NMR of <b>73</b> .....	32

## List of Tables

<b>Table 1</b> Proton NMR Comparison of <b>73</b> .....	31
<b>Table 2</b> Reaction conditions of cyclopropanation of <b>84</b> .....	34
<b>Table 3</b> Halogenation reaction conditions completed with <b>85</b> .....	34



## List of Schemes

<b>Scheme 1</b> Conversion of salicin to salicylic acid; acetylation of salicylic acid .....	4
<b>Scheme 2</b> Semi-synthesis of Taxol.....	6
<b>Scheme 3</b> Conversion of ammonium cyanate to urea via Wohler Synthesis .....	6
<b>Scheme 4</b> Retrosynthetic analysis of lagunamide A, adapted from Dai. ....	15
<b>Scheme 5</b> Synthesis of lagunamide A polyketide fragment, adapted from Dai. ....	16
<b>Scheme 6</b> Alternative route towards <b>19</b> .....	17
<b>Scheme 7</b> Deconstruction of <b>15.1</b> adapted from Pal and Chakraborty.....	19
<b>Scheme 8</b> Synthetic route of polyketide <b>47</b> of <b>15.1</b> adapted from Pal and Chakraborty .....	20
<b>Scheme 9</b> Lagunamide C deconstruction .....	22
<b>Scheme 10</b> Retrosynthetic analysis of <b>57</b> .....	23
<b>Scheme 11</b> Module I: Setting the first stereocenter via titanium-mediated mixed aldol .....	24
<b>Scheme 12</b> Equivalent control of TiCl <sub>4</sub> , adapted from Hodge and Olivio and Crimmins. ....	24
<b>Scheme 13</b> Module II: Stereospecific cyclopropanation via dioxaborolane catalysis .....	25
<b>Scheme 14</b> Module III: Stereoselective reduction to achieve the third stereocenter .....	26
<b>Scheme 15</b> Proposed transition state of CBS reduction as adapted from Corey and Halal. ....	26
<b>Scheme 16</b> Proposed terminal alkene vs methyl-truncated terminal alkene.....	28
<b>Scheme 17</b> Formation and acetylation of <b>77</b> .....	29
<b>Scheme 18</b> Titanium-mediated mixed aldol reaction.....	30
<b>Scheme 19</b> TBS protection and reductive cleavage of <b>73</b> .....	32
<b>Scheme 20</b> Oxidation, Wittig olefination, DIBAL-H reduction.....	33
<b>Scheme 21</b> Model system of cyclopropanation and halogenation using <b>84</b> .....	33
<b>Scheme 22</b> Cyclopropanation, iodine substitution of <b>83</b> .....	35

<b>Scheme 23</b> Charette ring-opening of <b>88</b> .....	35
---	----

## Abbreviations

<b>μM</b>	micromolar
<b>1-NMP</b>	1-methyl-2-pyrrolidinone
<b>2,2-DMP</b>	2,2-dimethoxypropane
<b>BF<sub>3</sub>-OEt<sub>2</sub></b>	boron trifluoride diethyl etherate
<b>Bu<sub>2</sub>BOTf</b>	dibutylboryl trifluoromethanesulfonate
<b>CAN</b>	ceric ammonium nitrate
<b>CBS</b>	Corey-Bakshi-Shibata
<b>CH<sub>2</sub>Cl<sub>2</sub></b>	dichloromethane
<b>CH<sub>2</sub>I<sub>2</sub></b>	methylene iodide
<b>CH<sub>3</sub>COCl</b>	acetyl chloride
<b>C-NMR</b>	carbon nuclear magnetic resonance
<b>CS<sub>2</sub></b>	carbon disulfide
<b>CSA</b>	camphorsulfonic acid
<b>d</b>	doublet
<b>dd</b>	doublet of doublets
<b>DCM</b>	dichloromethane
<b>DDQ</b>	2,3-dichloro-5,6-dicyano-1,4-benzoquinone
<b>DIBAL-H</b>	diisobutylaluminum hydride
<b>DIPEA</b>	diisopropylethyl amine
<b>DMF</b>	dimethyl formamide
<b>DMP</b>	Dess-Martin Periodane
<b>DMSO</b>	dimethyl sulfoxide
<b>eq.</b>	equivalent
<b>Et<sub>2</sub>O-MeOH</b>	diethyl ether-methanol
<b>Et<sub>2</sub>Zn</b>	diethyl zinc
<b>Et<sub>3</sub>N</b>	triethyl amine
<b>EtOH</b>	ethanol
<b>g</b>	grams
<b>H</b>	hydrogen
<b>H<sub>2</sub>O</b>	water
<b>H<sub>2</sub>O<sub>2</sub></b>	hydrogen peroxide
<b>HCl</b>	hydrochloric acid
<b>HF</b>	hydrofluoric acid
<b>HRMS</b>	high resolution mass spectroscopy
<b>H-NMR</b>	hydrogen nuclear magnetic resonance
<b>IC<sub>50</sub></b>	half maximal inhibitory concentration
<b>J</b>	J-couplings
<b>KOBut</b>	potassium butoxide

<b>KOH</b>	potassium hydroxide
<b>LDA</b>	lithium diisopropylamide
<b>LiAlH<sub>4</sub></b>	lithium aluminum hydride
<b>LiCl</b>	lithium chloride
<b>M</b>	molar
<b>m</b>	multiplet
<b>MeCN</b>	methyl cyanide
<b>MeOH</b>	methanol
<b>mg</b>	milligram
<b>MHz</b>	megahertz
<b>mL</b>	milliliter
<b>mmol</b>	millimole
<b>Na<sub>2</sub>CO<sub>3</sub></b>	sodium carbonate
<b>NaHCO<sub>3</sub></b>	sodium bicarbonate
<b>NaIO<sub>4</sub></b>	sodium iodate
<b>NaOH</b>	sodium hydroxide
<b>n-Buli</b>	n-butyl lithium
<b>NH<sub>4</sub>Cl</b>	ammonium chloride
<b>nM</b>	nanomolar
<b>O/N</b>	over night
<b>OBn</b>	benzyl ether
<b>OMTM</b>	methylthiomethyl ether
<b>OsO<sub>4</sub></b>	osmium tetroxide
<b>p</b>	pentet
<b>Pd/C</b>	palladium over carbon
<b>PivCl</b>	pivaloyl chloride
<b>PPTS</b>	pyridinium p-toluenesulfonate
<b>PTSA</b>	p-toluenesulfonic acid
<b>Py</b>	pyridine
<b>pySO<sub>3</sub></b>	pyridine sulfite
<b>RT</b>	room temperature
<b>SM</b>	starting material
<b>s</b>	singlet
<b>TBS</b>	tertbutyldimethylsilane
<b>TBSCl</b>	tertbutyldimethylsilyl chloride
<b>TEA</b>	triethyl amine
<b>TESOTf</b>	triethylsilyl trifluoromethanesulfonate
<b>THF</b>	tetrahydrofuran
<b>TiCl<sub>4</sub></b>	titanium tetrachloride
<b>TMEDA</b>	tetramethyl ethylene diamine
<b>t</b>	triplet

## **Acknowledgements**

I would like to acknowledge my brilliant lab mates and Dr. Ryan Rafferty for their support and guidance throughout my graduate career. I am also grateful for my committee members, Dr. Hua and Dr. McLaurin for their patience, knowledge, and support. Finally, I wish to acknowledge my husband, Josh, for his endless support whilst I was working in the lab late at night and taking so long to write this thesis.

## **Dedication**

I wish to dedicate this work to my parents, Julie and Rodd. Your love and encouragement has inspired me to become a better scientist

# Chapter 1 - Introduction to Natural Products

## 1.0 Introduction

Humans have been taking advantage of nature's organisms for millennia. <sup>1</sup> Tea has been used in Asian civilizations for over 4,000 years as a social beverage, remedy for ailments, and carries ceremonial significance. <sup>2</sup> The aloe vera plant has been used all over the world to soothe burns and skin irritation and to treat constipation. <sup>3</sup> South American cultures use coca leaves to soothe toothaches, headaches, and altitude sickness. <sup>4</sup> Honey is used as a natural sweetener, antibiotic, and as treatment for the common cold. <sup>5</sup> These natural products are derived from all walks of life including plants, animals, insects, and microbes. While seemingly ordinary, these resources provide an arsenal of compounds for treating disease.

These natural products, equipped with unmatched structural and chemical biodiversity, have been evolutionarily optimized has secondary metabolites for the host organism. <sup>6</sup> Secondary metabolites are compounds that are not directly involved with the growth, reproduction, or development of an organism, and are often involved with developments such as unique defense mechanisms, sexual hormones, and differentiation. <sup>6</sup> An example of secondary metabolites can be found in some species of cold water fish. These organisms contain "anti-freeze" proteins that enable them to thrive in extremely cold conditions by preventing the water in cells from freezing and bursting. <sup>7</sup>

Scientists have found secondary metabolites to contain medicinal, cosmetic, and nutritional properties of interest for human use. Common examples of secondary metabolites include Botox, recognized for its ability to treat at least 50 types of smooth muscle conditions, the analgesic aspirin, and the primary drug for treating breast and ovarian cancers, Taxol.

### 1.0.1 Botox

*Clostridium botulinum* is the gram-positive food-borne bacteria infamous for botulism and is currently one of the deadliest neurotoxins on earth with  $IC_{50}$  values of 1-2  $\mu\text{g}/\text{kg}$  in humans.<sup>8</sup> These effects are caused by seven neurotoxins, A-H, produced by the bacteria. The toxin works by binding to recognition sites in muscle cells and decreases the release of acetylcholine, thereby causing a temporary neuromuscular blockage.<sup>8,9</sup> Arresting the release of acetylcholine prevents the muscles from contracting, and becomes deadly when respiratory and cardiac muscles are paralyzed.<sup>10</sup> Botulinum toxin A, shown in **Figure 1**, is the most potent form and is currently the only form of the toxin commercially available for pharmaceutical use.<sup>9,10</sup>

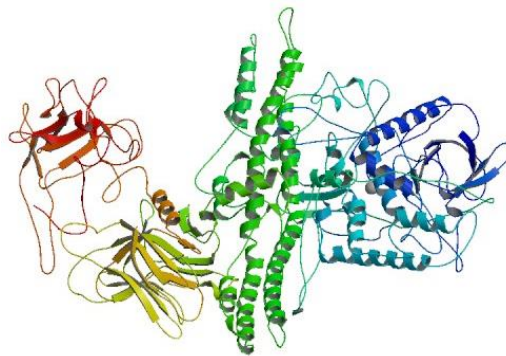


**Figure 1** Quaternary Structure of Botulinum Toxin A<sup>11</sup>

Originally, it was thought that botulinum toxin was spread through the consumption of specific foods, such green beans; however, in the early 1900's, it was found that the poison was a result of improper food preservation methods.<sup>8</sup> Medicinal use of botulinum toxin was not employed until the mid-1970's after a study completed by an ophthalmologic surgeon, Alan B. Scott, found that if picograms of botulinum toxin was administered to a subject, the toxin remained relatively localized to the injection site, and therefore produced localized paralysis.<sup>8</sup> This ground breaking discovery lead to treating a variety of conditions including strabismus and hyperactive sweating.



Botulinum toxin A is prepared for clinical use by isolating the toxin from *C. botulinum* cultures. It is then diluted with albumin, bottled, and lyophilized.<sup>9</sup> Botulinum toxin A has been employed to treating several conditions including focal dystonias, smooth muscle hyperactive disorders, overactive bladder disorders, and cerebral palsy.<sup>8</sup> In the early 2000's, the toxin was FDA approved for the prevention and treatment for facial wrinkles induced by aging. This method of administering the toxin is now commonly known as Botox.<sup>8,9</sup>

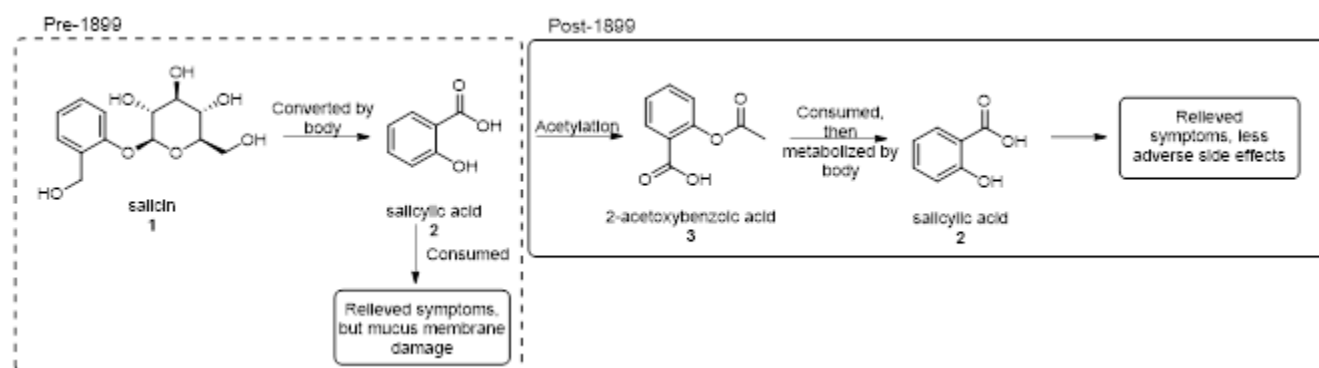
### 1.0.2 Aspirin

Another well-known natural product is the household analgesic aspirin - one of the most common substances used in modern medicine. This compound, derived from willow tree bark, has been used to relieve pain for thousands of years.<sup>12</sup> The first documented use dates back 4000 years by the Sumerians.<sup>12, 13</sup> Historical figures, including Hippocrates and Dioscorides, attribute pain relieving and anti-inflammatory properties to orally administered willow tree bark.<sup>14</sup>

While the medicinal benefits of willow tree bark were recognized, the drug was first chemically investigated in the early 19th century. Powder from willow tree bark was administered to patients in the first clinical studies completed by Reverend Edward Stone.<sup>12</sup> Over time, patients found that using the drug was an effective pain reliever, but they experienced severe pain and irritation towards mucus membranes. The active chemical derived directly from willow tree bark, salicin (**1**), as shown in **Scheme 1**, was isolated by Johann Buchner in 1828, and the pure crystalline form of salicin was isolated by Henri Leroux in 1829.<sup>12, 14</sup> Large scale production of salicylic acid (**2**) began in the late 1800's and became available for medicinal use.<sup>14</sup>

While many patients experienced pain relief from salicylic acid, it came at a cost. Regular use of salicylic acid left patients with painful gastrointestinal irritation and damage. It was found that the body metabolizes salicin into salicylic acid, the chemical responsible for the mucosal

membrane irritation, thus limiting its beneficial effects.<sup>14</sup> A new drug with less severe side effects was necessary.



**Scheme 1** Conversion of salicin to salicylic acid; acetylation of salicylic acid

Felix Hoffman was given the task of finding a drug that served as a pain reliever, anti-inflammatory, and fever reducer, but did not cause adverse side effects.<sup>12</sup> The solution was found via the acetylation of salicylic acid. This acetylated form of the drug still served as a pain reliever, but did not have the adverse side effects that were produced by salicylic acid alone. When administered, acetylated salicylic acid (3) is metabolized back into salicylic acid and used by the body as shown in **Scheme 1**.<sup>14</sup> In 1899, this new acetylated drug was entitled “Aspirin” by The Bayer Company, and became available without a prescription in 1915.<sup>14</sup> Over 100 years later, this naturally-derived drug is still used as a pain reliever, anti-inflammatory agent, and blood thinner without inducing adverse side effects.

### 1.0.3 Taxol

Like aspirin, paclitaxel (also known as Taxol, illustrated in **Figure 2**, is a natural product derived from tree bark.<sup>16</sup> Taxol (4) was isolated from the yew tree, *T. brevifolia*, by the US National Institute of Health in 1966 during a plant screening program and was later found to be potent IC<sub>50</sub> values towards a variety of cancer cell lines including HeLa (cervical, 2.6 nM), A549 (lung, 4.1 nM), U373 (Grade III astrocytoma, 4.2 nM), MCF-7 (breast, 2.5 nM), HT-29 (colon, 2.8 nM),

OVG-1 (ovarian, 4.0 nM), PC-Sh (pancreatic, 7.5 nM), and and PC-Zr (pancreatic, 4.0 nM).<sup>15</sup> The structure was elucidated in 1977 and clinical trials were approved for treating cervical cancer in 1993, causing a great demand for this compound.<sup>16</sup>

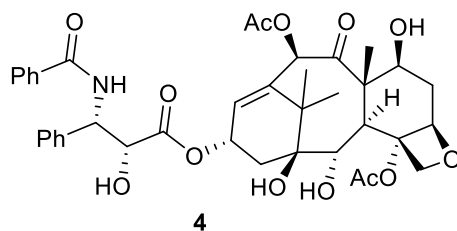
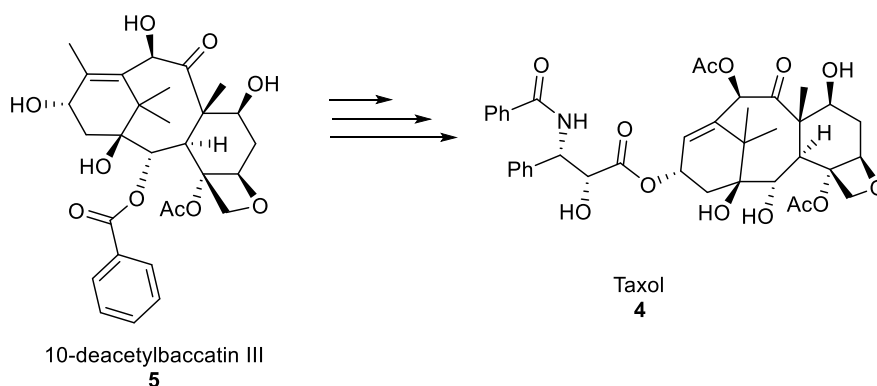


**Figure 2** Structure of Taxol

As a viable treatment for several types of cancer, Taxol was vital, but obtaining it proved challenging.<sup>17</sup> While the compound can be extracted from the yew tree, the overall yield from extraction is very low, 0.02% overall yield.<sup>17</sup> Obtaining a gram of Taxol would require the bark of approximately three yew trees.<sup>17</sup> This method also posed a problem for the survival of the yew tree, as the tree dies following the harvest of the bark. The cost of formulating Taxol directly from the bark was very high, costing ten times the allotted budget of the screening project.<sup>17</sup> A more efficient method of obtaining this valuable compound was significantly necessary in order to produce the drug on a larger scale to satisfy high demand of the compound.

Several methods were tested to obtain mass quantities of Taxol, including farming, cell culture, semi-synthesis and total synthesis.<sup>16</sup> The semi-synthesis of Taxol, shown in **Scheme 2**, involved extracting starting material, 10-deacetylbaccatin III, from a shrub, *T. baccata*, and then, via synthetic manipulations, acquire the desired compound.<sup>17, 18</sup> Ultimately, Taxol would need to be synthesized in order to obtain enough of the compound to be clinically administered to cancer patients.

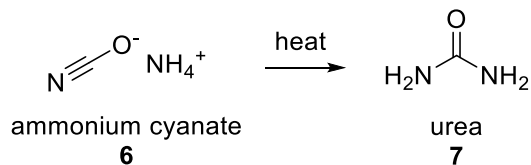


### **Scheme 2** Semi-synthesis of Taxol

The total synthesis of Taxol was achieved in two years by Nicolau *et. al* in 1995, nearly thirty years after its original discovery.<sup>16</sup> It was important to have a relatively short, manipulative, synthetic route that not only produced Taxol, but analogs of the compound throughout the process. The synthesis took over 40 steps and involved key reactions including a Shapiro Reaction, McMurry Coupling, and Sharpless Epoxidation with an overall yield of less than 0.1 %.<sup>16</sup> The total synthesis of Taxol has allowed for obtaining enough of the compound to use in medicine without completely depleting the natural source.

### **1.1 Total synthesis**

Friedrich Wöhler, a German chemist, is attributed for synthesizing the first organic compound, urea (**7**), as shown in **Scheme 3**, through the heating of ammonium cyanate (**6**).<sup>19</sup> His discovery refuted the “vitalism hypothesis” thus proving that organic compounds can be synthesized from inorganic chemicals.<sup>20</sup>



### **Scheme 3** Conversion of ammonium cyanate to urea via Wohler Synthesis

This method of generating materials, termed total synthesis, has exploded, resulting in the synthesis of thousands of compounds ranging across various disciplines in society.<sup>20</sup> Dyes, polymers, cosmetics, textiles, pesticides, and pharmaceuticals are a small handful of products made available by total synthesis.<sup>20</sup>

The Wohler Synthesis of urea initiated the synthesis of thousands of compounds, including secondary metabolites with medicinal properties such as aspirin, and Taxol.<sup>20</sup> With the exception of botulinum toxin A, extracting the compounds from their natural sources is neither economical, nor ecologically feasible. Salicin (**1**) extracted directly from the willow tree must first be formed into salicylic acid and then acetylated into its most usable form. The yew tree, *T. brevifolia*, is slow growing, relatively rare, and considered an endangered species.<sup>17</sup> In order to obtain enough of the respective compounds from their natural sources, their natural source would be completely depleted and dramatically increase the cost of the drug. Issues like this can be resolved through total synthesis. This process allows scientists to obtain these compounds without depleting their natural sources and allows for stereochemical modifications of the compounds for medicinal use.

This method of production is not without caveats, as it is often a lengthy, synthetically challenging, and expensive process.<sup>20</sup> Complicated structures often require more steps with more care placed towards facial selectivity. However, synthesizing complex structures can have beneficial biological and chemical implications that make the process rewarding.<sup>20</sup> For example, the total synthesis of Taxol was revolutionary in the field of synthetic chemistry, and is used to help treat several types of cancer. Conversely, producing Taxol on a large scale via total synthesis is problematic.

Total synthesis can lead the scientific community to question the necessity of this method as it is often an expensive and lengthy process that is not necessarily feasible towards mass

production. For instance, a total synthesis for aspirin and Taxol, among thousands of other medicinally important compounds, have been completed, but, are not necessarily the way in which mass quantities of the drug are obtained. Taxol is currently produced semi-synthetically. An important aspect of total synthesis is that it allows for the formation of non-natural derivatives of compounds that could provide new drug leads.<sup>1</sup>

## 1.2 Natural products and cancer

Cancer is one of the most notorious diseases known to mankind and is the second leading cause of death in the United States.<sup>21</sup> It is estimated that more than 600,000 people will die and over 1.6 million new cases of cancer will be diagnosed in 2017 alone.<sup>21</sup> Apart from practicing preventative health measures, such as eating a healthy diet and exercising, new drug leads are necessary to fight this disease. Discovering and synthesizing new natural products may be key to fighting cancer.

Since the 1940's, over 75% of anticancer drugs have been inspired by natural products found in both terrestrial and marine sources.<sup>23</sup> Earth's oceans have been a leading source for natural products and recent advances in technology allow for scientists to explore areas of the ocean once deemed "unreachable". Since 2012, over 1100 new marine natural products have been documented and thirteen of these are currently undergoing the final stages of clinical trials.<sup>22, 23</sup> Nine have been approved for medicinal use and include cytarabine (Ara-C), trabectedin (**8**), halichondrin B, and auristatin E.<sup>23</sup>

These compounds are derived from a variety of marine organisms, including sponges, tunicates, sea hare and invertebrates such as proferia and cnidaria.<sup>23</sup> Dolastatins (**8**) are compounds derived from cyanobacterium and are currently undergoing trials for the treatment of melanoma.<sup>23</sup> A broad-spectrum cancer drug, trabectedin (**9**), is derived from the tunicate, *Ecteinascidia*

*turbinata*. This drug interacts with the minor grooves of DNA and interferes with transcription, repair mechanisms, and cellular division.<sup>23</sup> A synthetic analog of phenylahisitin, Plinabulin (**10**), is derived from the marine fungus, *Aspergillus*, and impedes tumor growth via the inhibition of tubulin polymerization, inducing apoptosis, and disrupting the vasculature of the tumor.<sup>23</sup> These three compounds are illustrated in **Figure 3**.

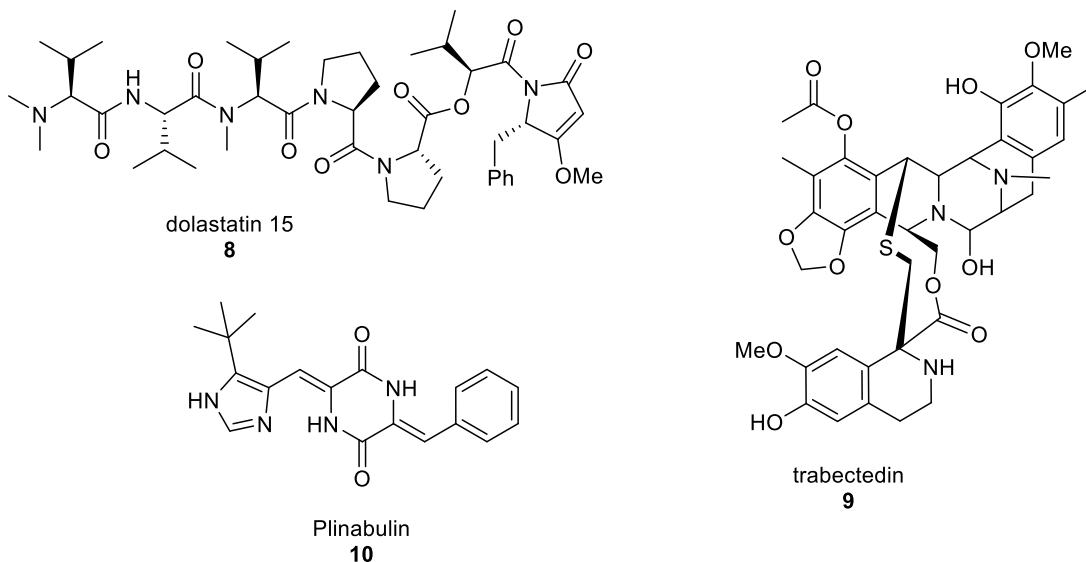


**Figure 3** Cancer-fighting natural products derived from marine organisms

Another family of compounds with specific interest for cancer therapy are the aurilides. These depsipeptides, originally derived from sea hare, and are currently being investigated for cancer therapy as they often have toxicity values in the picomolar to nanomolar range.<sup>24</sup> Aurilides are macrocyclic compounds containing amino acids. Compounds that belong to the aurilide family include aurilides A, B, and C, paul'au amide, and kulokehahilide-2.<sup>25</sup> The lagunamides are structurally similar to aurilides and are also categorized as depsipeptides. Structural similarities

between aurilides and lagunamides, along with their respective IC<sub>50</sub> values, are shown in **Figure**

4.

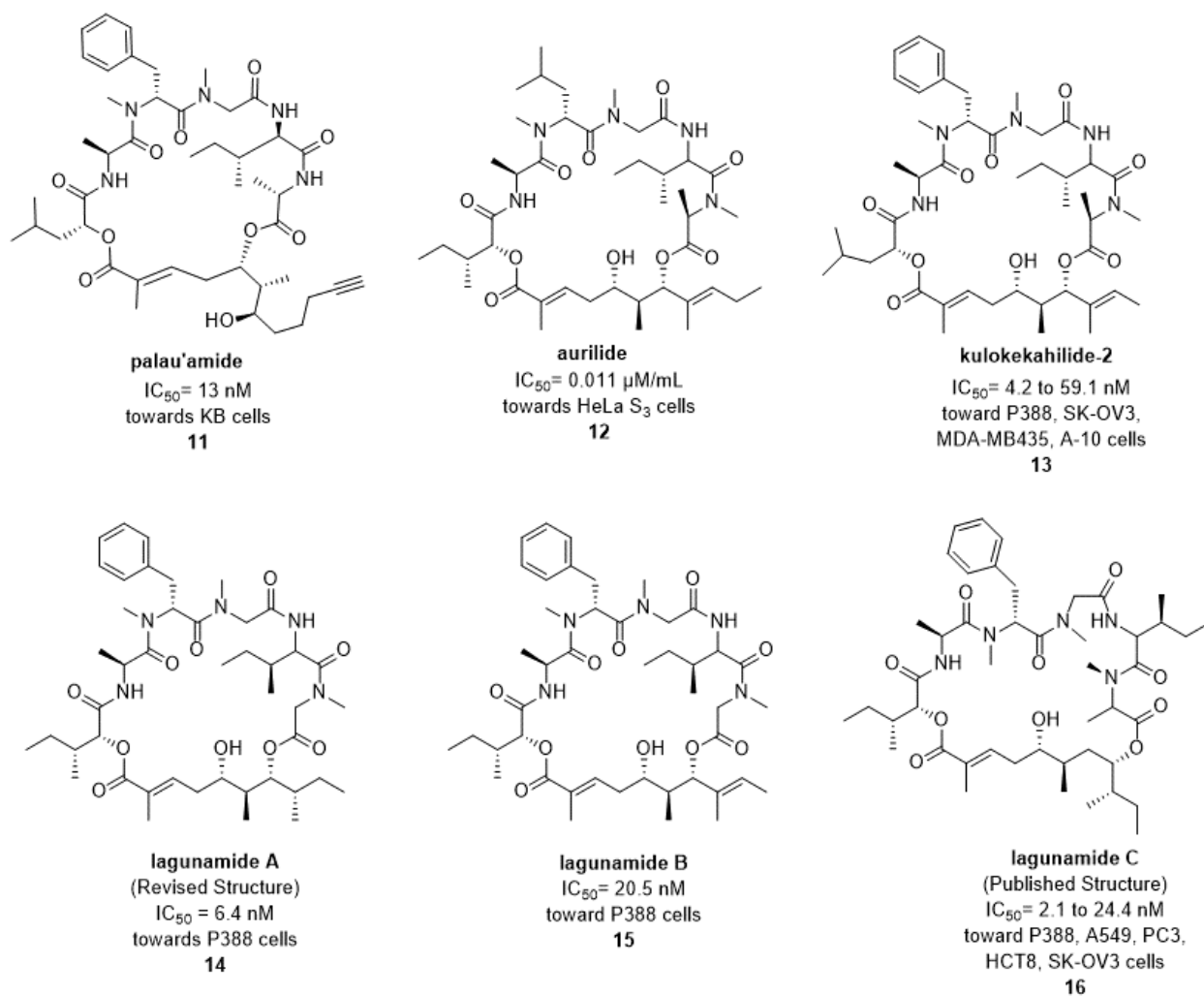


**Figure 4** Structures and IC<sub>50</sub> values of select aurilides and lagunamides

Secondary metabolites from marine cyanobacteria have also been proven to be of interest due to their unique antimalarial and anticancer properties.<sup>26</sup> Lagunamide A (**14**), lagunamide B (**15**), and lagunamide C (**16**) are secondary metabolites that were first isolated from the cyanobacterium *Lyngbya majuscula* by Tan *et al.* from Palau Hantu Besar, Singapore in 2007.<sup>25</sup> Each compound was tested for cytotoxicity and showed impressive antimalarial and anticancer activities through mitochondrial-mediated apoptosis.<sup>26</sup> Lagunamides A and B showed IC<sub>50</sub> values of 0.19 μM and 0.91 μM, respectively, for antimalarial activity. Lagunamide C has shown



anticancer activity, as such by its IC<sub>50</sub> values, towards an array of cancer cell lines including P388 (leukemia, 24.4 nM), A549 (lung, 2.4 nM), PC3 (prostate, 2.6 nM), HCT8 (colon, 2.1 nM), and SK-OV3 (ovarian, 4.5 nM).<sup>25,26</sup>

Similar to aurilides, the lagunamides have a polypeptide backbone, composed of five amino acids, and a polyketide fragment. The pentapeptide backbone is very similar in lagunamides A, B, and C; however, each lagunamide has a unique polyketide fragment. These differences may be the cause of the differing toxicities associated with each lagunamide. The synthesis of Lagunamide A and an analog of lagunamide B have been reported and the total synthesis of lagunamide C and an analog of lagunamide C is currently underway.<sup>27, 28</sup> These synthetic routes will be discussed in Chapter 2.

### **1.3 Summary**

Natural products are derived from many types of organisms and are useful in treating various conditions including neuromuscular disorders, pain, and cancer.<sup>6, 8, 9, 14, 18</sup> Extraction of these compounds from their natural sources is often not ecologically nor economically feasible, and therefore can be produced synthetically.<sup>1, 17, 20</sup> This method may be questioned by the scientific community as it is a lengthy, and often expensive, process.<sup>1, 20</sup> Total synthesis offers benefits that include producing compounds not naturally produced in nature and confident structural elucidation.

Cancer-fighting natural products have been extracted from marine sources.<sup>22, 23, 24, 26</sup> Total synthesis has made many of these compounds available for pharmaceutical use.<sup>22, 23, 24, 26</sup> Lagunamides A, B, and C have shown impressive cytotoxicities towards a variety of cancer cell lines. The synthesis of Lagunamide A and an analog of lagunamide B have been reported and it was proven that the original structures produced by the isolation team were incorrect.<sup>27, 28</sup>

Lagunamide C has yet to be synthesized and its structure confidently elucidated. To be delineated herein are the efforts of developing a tunable route to obtain lagunamide C.

## Chapter 2: Previous Synthesis and Proposed Work

### 2.0 Previous Synthetic Work

The total syntheses of lagunamide A (**14**) and an analog of lagunamide B (**15.1**) have been reported.<sup>27, 28</sup> Dissection of both compounds break them into a polypeptide backbone and a polyketide fragment (highlighted in green in **Figure 5**). Lagunamides A, B, and C share structurally similar polypeptide backbones and can be synthesized by a series of peptide couplings. The focus will be on the synthesis of the polyketide fragments within the compounds. The polyketide fragments differ in all three compounds, and it is proposed that this moiety could be related to the varying toxicities associated with each lagunamide. The differences within the polyketide moieties (shown in green) of the lagunamides are highlighted in **Figure 5** in the red

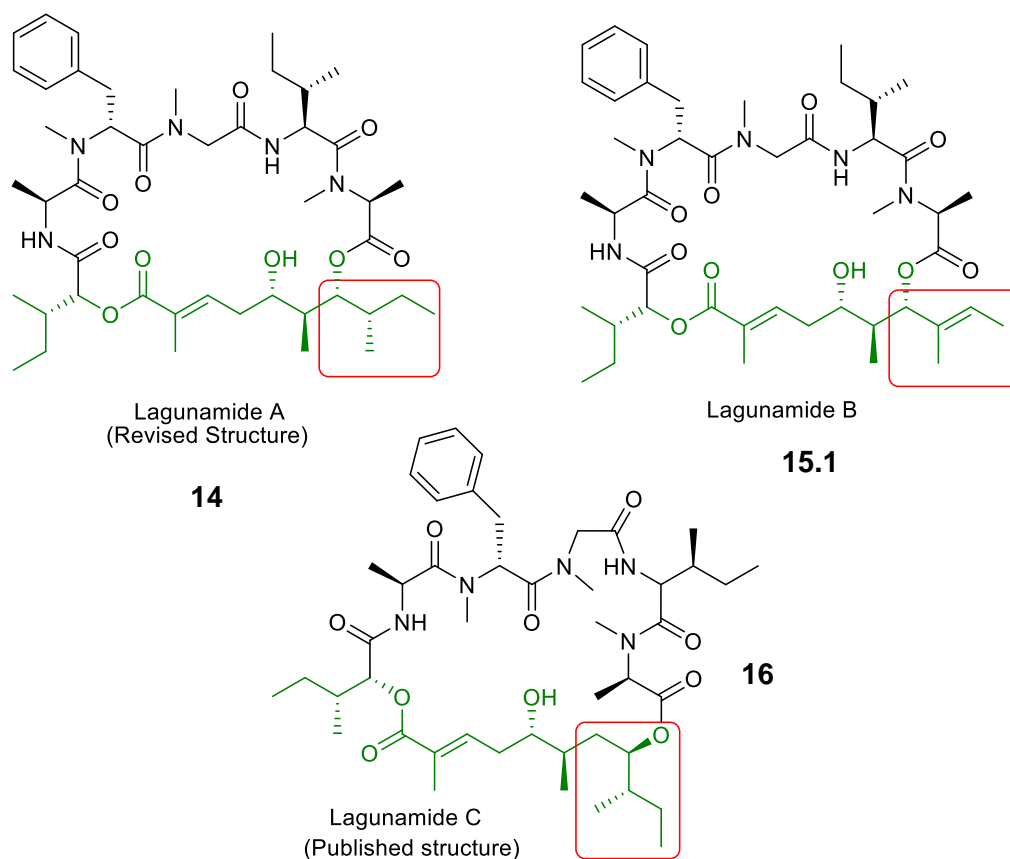


**Figure 5** Polyketide fragments of lagunamides A, B, and C

boxes.<sup>25, 26, 29</sup> While lagunamide A and lagunamide C are almost structurally identical, the crotylation techniques employed for the synthesis of lagunamide A are not applicable in synthesizing the polyketide fragment of lagunamide C due to the addition of one carbon in the polyketide fragment of lagunamide C. This, in addition to the stereochemical inaccuracies, validates the necessity of a new synthetic route to obtain lagunamide C.

### 2.0.1 Synthesis of lagunamide A

The structure of lagunamide A was elucidated by the isolation team via intense spectroscopic methods.<sup>27</sup> After the total synthesis was completed, it was found that the previously elucidated structure was incorrect initially due to skepticism related to the “anticipated common bacterial biogenesis of related marine nature products.”<sup>27</sup> The stereochemical assignment of C39 was identified as *S* but proven to be *R* via total synthesis of diastereomers of the compound. The spectra of the diastereomers was compared to that of the original isolated compound and it was found that the C39 stereochemistry was indeed assigned incorrectly, as illustrated in **Figure 6**.

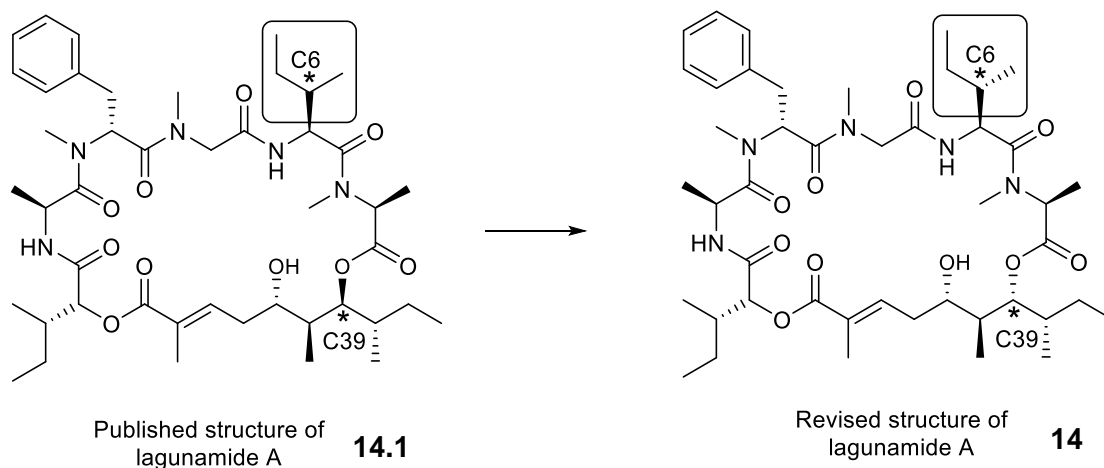
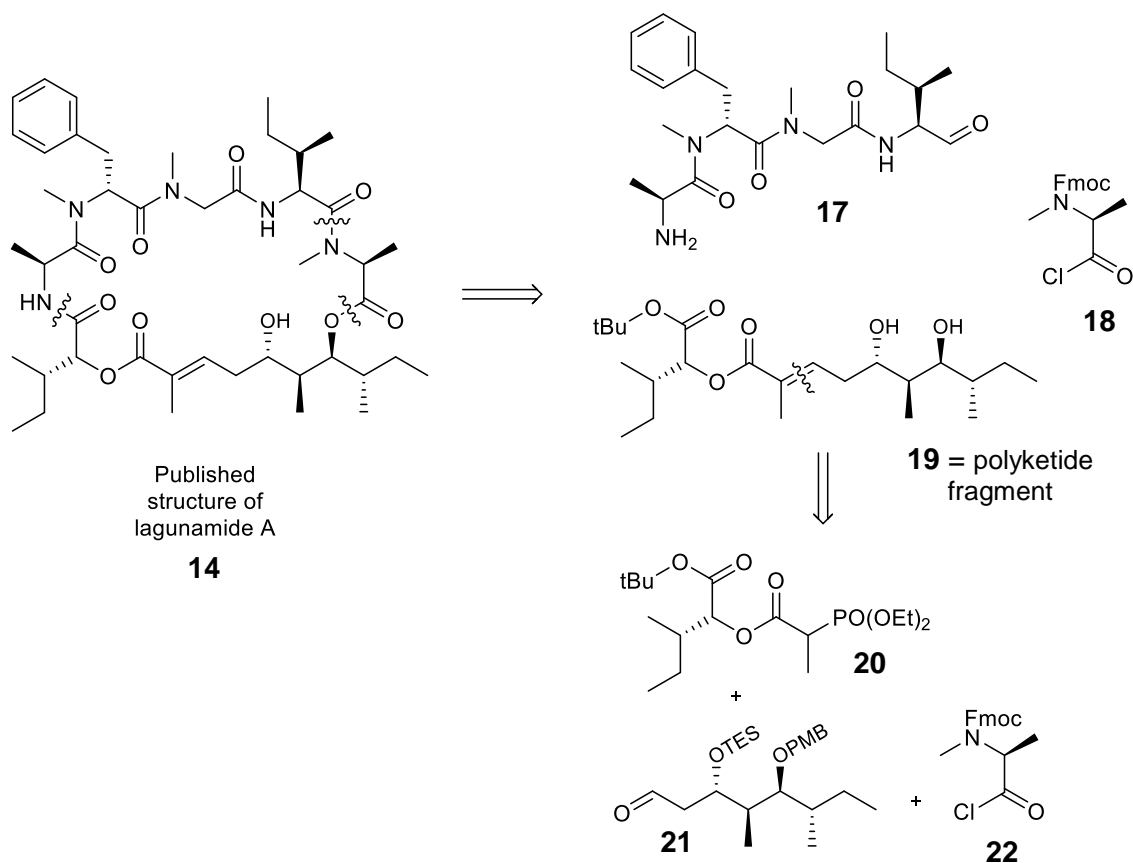


**Figure 6** Published and revised structures of lagunamide A<sup>27</sup>

The total synthesis and stereochemical revision of lagunamide A was completed in 2012 by Dai and coworkers.<sup>27</sup> The compound is composed of 11 stereogenic centers, 8 of which are

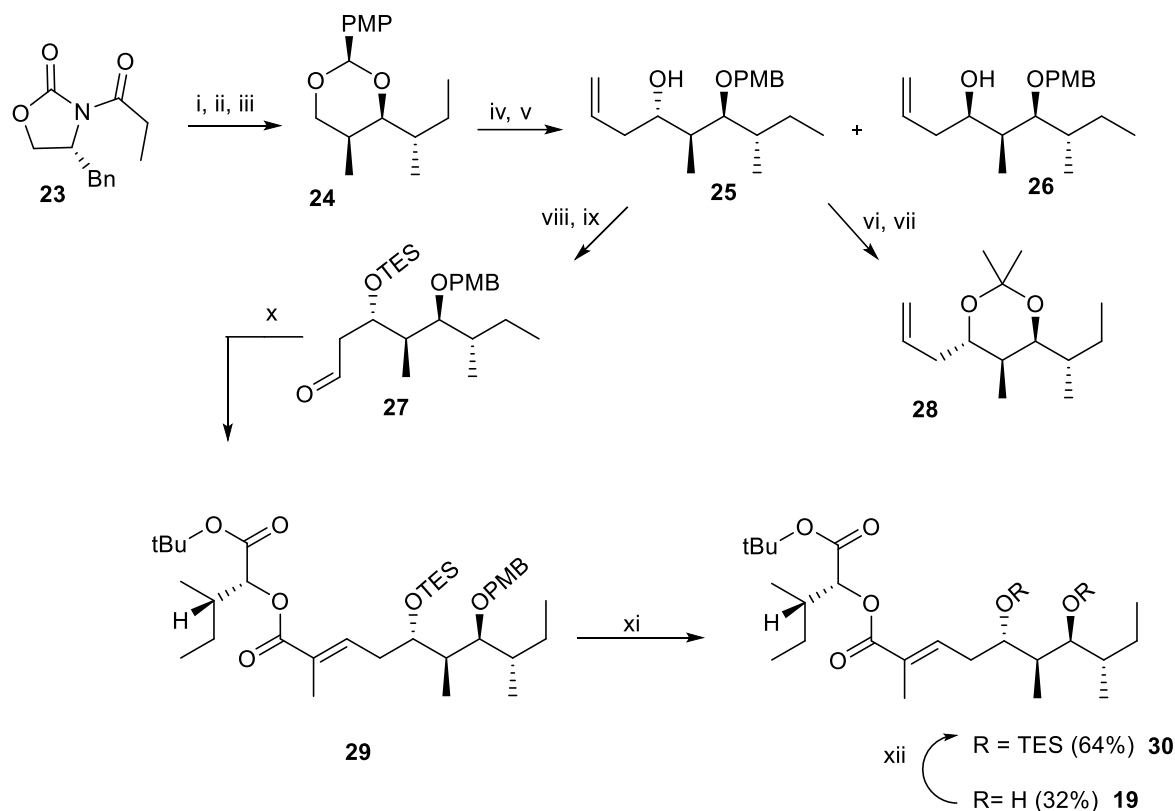
found within the pentapeptide backbone, as shown in **Scheme 4**.<sup>27</sup> The synthesis of the polyketide fragment of lagunamide A features a chiral auxiliary, DIBAL-H reductive cleavage, diastereoselective allylation, and oxidative cleavage.



**Scheme 4** Retrosynthetic analysis of lagunamide A, adapted from Dai.<sup>27</sup>

The synthesis of the polyketide fragment of lagunamide A, illustrated in **Scheme 5**, was initiated by treating the modified Evans (*R*)-oxazolidinone, (**23**), with (*S*)-2-methyl butanal to give the corresponding alcohol. The alcohol was subsequently converted into anisylidene acetal (**24**) in a two-step process via NaBH<sub>4</sub> reductive elimination.<sup>27</sup> The diol was then subjected to acetylation followed by a DIBAL-H reduction of the acetal to the primary alcohol. The remaining alcohol was then subjected to a Dess-Martin oxidation to afford the aldehyde that then underwent diastereoselective allylation via Keck's protocol to produce homoallylic alcohols in an

anti-syn ratio of 7:3 (**25** and **26**). The homoallylic alcohol was then protected via TES ether and subjected to an osmium tetroxide mediated oxidative cleavage, producing aldehyde **27**. The aldehyde was then homologated via Horner-Wadsworth-Emmons condensation and the diols were deprotected to afford compound **19**.

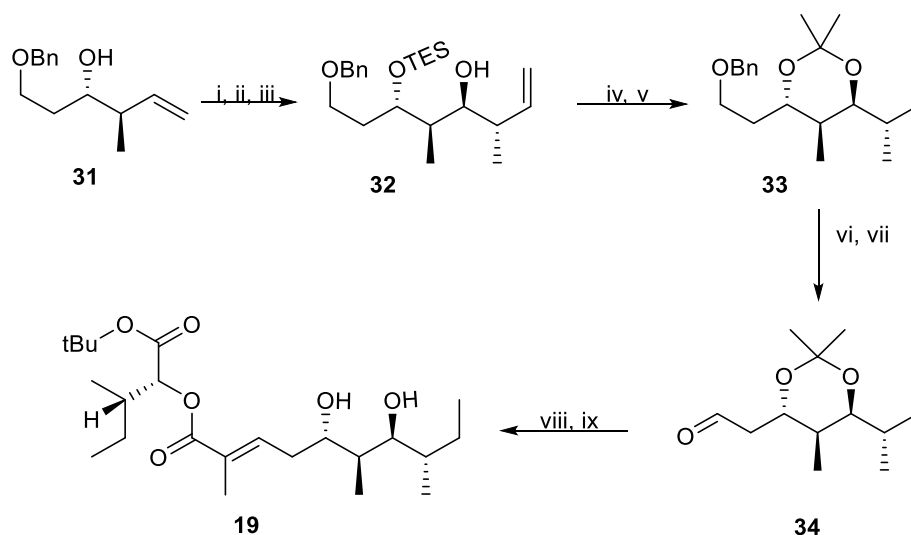


(i)  $\text{Bu}_2\text{BOTf}$ , DIPEA, DCM,  $0^\circ\text{C}$ ; then *S*-2-methylbutanal,  $-78^\circ\text{C}$ ; (ii)  $\text{NaBH}_4$ ,  $\text{Et}_2\text{O-MeOH}$ ; (iii) anisaldehyde dimethyl acetal, PPTS, DCM, 61%; (iv) DIBAL-H, DCM,  $-78$  to  $-10^\circ\text{C}$ ; (v) (a) Dess-Martin periodinane,  $\text{NaHCO}_3$ , DCM; (b) allyltributylstannane,  $\text{BF}_3\text{-OEt}_2$ , DCM,  $-78^\circ\text{C}$ ; (vi) DDQ, phosphate buffer; (vii) DMP, PTSA, 88%; (viii) TESOTf, 2,6-lutidine, DCM,  $-78^\circ\text{C}$ ; (ix)  $\text{OsO}_4$ ,  $\text{NaIO}_4$ , 2,6-lutidine, dioxane- $\text{H}_2\text{O}$ , 83%; (x) **20**, DIPEA, LiCl, MeCN, 84%; (xi) DDQ, phosphate buffer.

**Scheme 5** Synthesis of **30** adapted from Dai.<sup>27</sup>

The stereochemistry of the homoallylic alcohol was confirmed via observation of a respective acetonidization of the compound. The  $^{13}\text{C-NMR}$  spectra of the methyl groups of the acetonide showed characteristics of anti-1,3-diol. To ensure the integrity of the stereochemistry within the diol, an alternative approach, as shown in **Scheme 6**, was executed in which a

homoallylic alcohol (**31**) was TES protected (**32**), subjected towards oxidative cleavage, and then converted into the homoallylic alcohol via reagent controlled *anti*-crotylation. Following deprotection, the 1,3 diol was reprotected via acetonization to produce **33**. The alkene was hydrogenated and the resulting alcohol was oxidized to the corresponding aldehyde (**34**). The aldehyde was subjected to a Horner-Wadsworth-Emmons olefination with the desired phosphonate and the diols were deprotected. It was ultimately found that the diol's stereochemistry remained unchanged and identical to **19**; the deprotected form of **30** that was produced via the original method.



(i) TESOTf, 2,6-lutidine, DCM,  $-78^{\circ}\text{C}$ ; (ii)  $\text{OsO}_4$ ,  $\text{NaIO}_4$ , 2,6-lutidine, dioxane- $\text{H}_2\text{O}$ ; (iii) *E*-2-butene,  $\text{KO}^t\text{Bu}$ ,  $n\text{-BuLi}$ ,  $-78^{\circ}\text{C}$ , (-)- $\text{Ipc}_2\text{-BOMe}$ ,  $\text{BF}_3\text{OEt}_2$ ; then  $\text{Et}_3\text{N}$ ,  $\text{H}_2\text{O}_2$ , 62%; (iv)  $\text{HCl}$ ,  $\text{MeOH}$ ; (v) DMP, PPTS,  $60^{\circ}\text{C}$ , 89%; (vi)  $\text{H}_2$ ,  $\text{Pd/C}$ ,  $\text{MeOH}$ ; (vii) Dess-Martin periodane,  $\text{NaHCO}_3$ ,  $\text{DCM}$ , 92%; (viii) **20**, DIPEA,  $\text{LiCl}$ ,  $\text{MeCN}$ ; (ix) PTSA,  $\text{MeOH}$ , 81%

### Scheme 6 Alternative route towards **19**

After **19** was joined to the polypeptide backbone (**17**) and lagunamide A was synthesized, the authors noted that the synthesized structure “appeared epimeric to the proposed structure.”<sup>27</sup> At least two points in the macrocycle contained the incorrect configuration. Diastereomers were synthesized by preparing homoallylic alcohols from the common intermediate using the previous

protocol and  $^{13}\text{C}$ -NMR data of the synthesized compounds were compared to the originally isolated compound. This showed that while the C39 configuration was incorrect, there was another location, C6, within the macrocycle that required revision. The polypeptide portion was altered by replacing L-allo-isoleucine with L-isoleucine, and this, including the revision within the polyketide portion, produced the true configuration of lagunamide A, as previously shown in **Figure 6**.<sup>27</sup>

This stereochemical revision also impacts the stereochemical assignments within lagunamides B and C.<sup>27</sup> According to Tan and coworkers, Lagunamides A, B and C should have the same stereochemical assignment on C39. A total synthesis of lagunamides B and C are necessary to elucidate the correct structures of these compounds.

### 2.0.2 Synthesis of 15.1

Lagunamide B is composed of 10 stereogenic centers (7 from the amino acid backbone), a polyketide fragment, one hydroxyl acid, two L-amino acids, and three N-methyl amino acid residues in a 26-membered macrocycle.<sup>28</sup> An analog of lagunamide B (**15.1**), as illustrated in **Figure 7**, was synthesized by Pal and Chakraborty in 2014.<sup>28</sup>

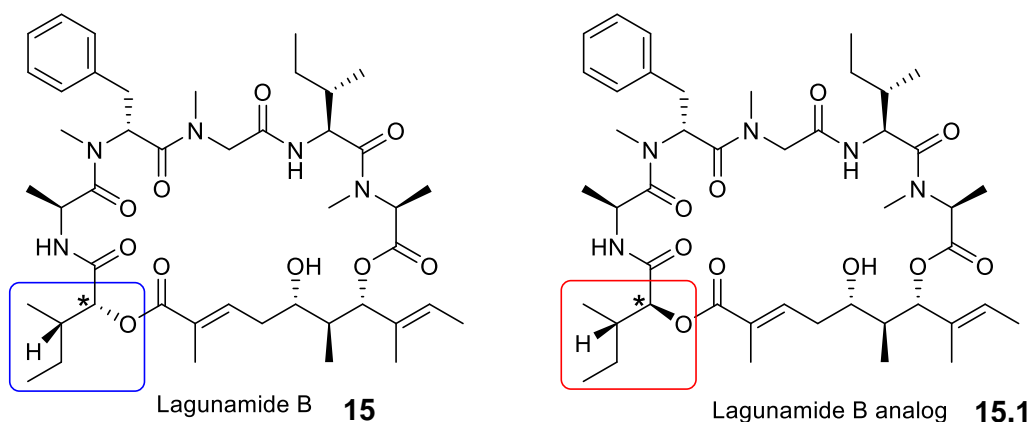
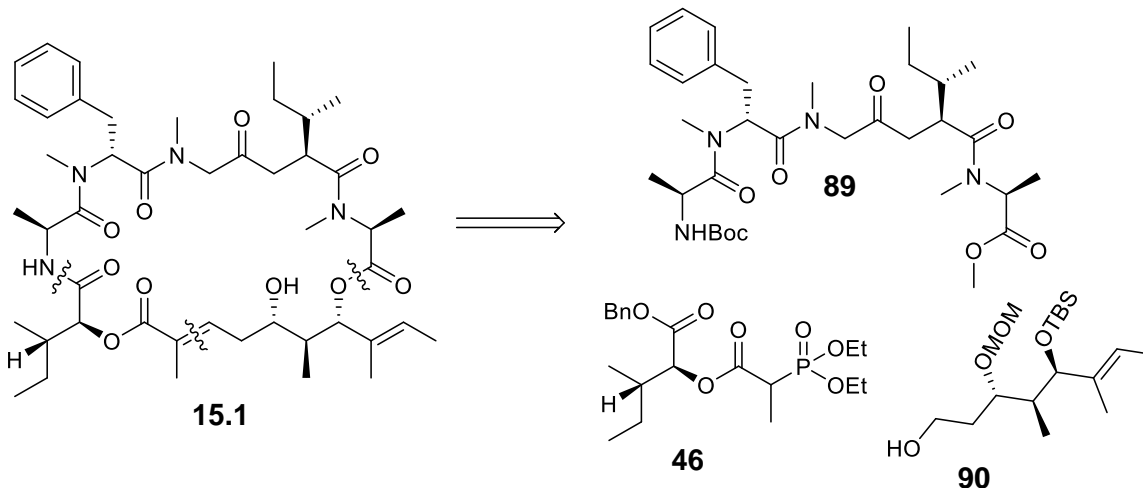


**Figure 7** Structures of lagunamide B and analog of lagunamide B





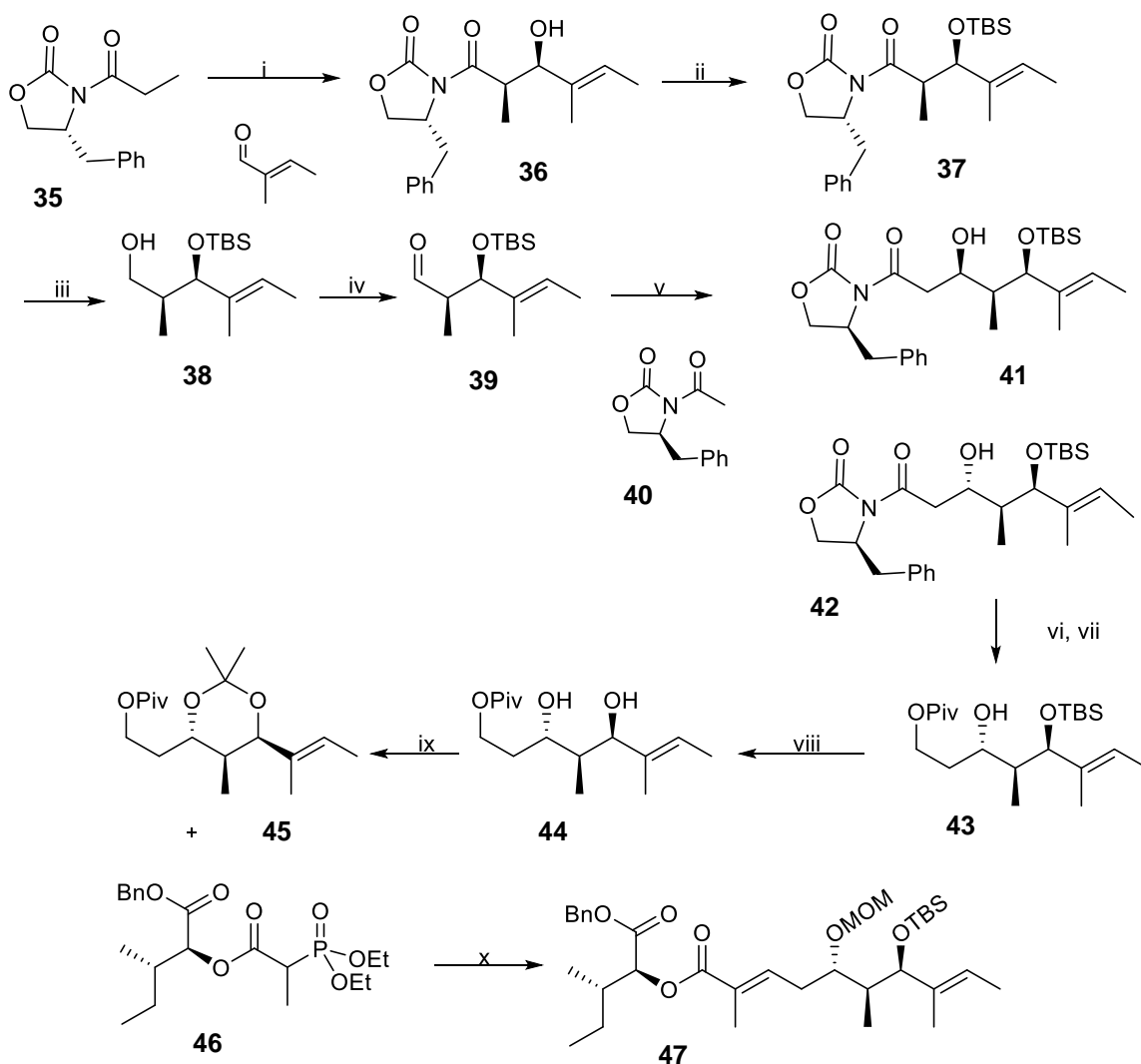
**Scheme 7** Deconstruction of **15.1** adapted from Pal and Chakraborty<sup>27</sup>

As in lagunamide A, the analog of lagunamide B (**15.1**) can be broken down into a polypeptide backbone (**89**) and polyketide fragment (**47**), as shown in **Scheme 7** and **Scheme 8**. The synthesis of the polyketide portion featured the use of two chiral auxiliaries and titanium-mediated mixed aldol reactions. The synthetic route is illustrated in **Scheme 8**.

As described by Pal and Chakraborty, the chiral auxiliary (**35**) was subjected towards a titanium-mediated mixed aldol reaction to produce **36** and then TBS protected to produce **37**. After the alcohol was protected, the compound was subjected towards lithium borohydride reduction to afford **38** followed by oxidation to produce **39**. Aldehyde **39** was then subjected towards a titanium-mediated mixed aldol reaction with auxiliary **40** to afford diastereomers **41** and **42**. With **42** in the desired conformation, it was subjected towards  $\text{LiBH}_4$  reduction to remove the auxiliary and then Piv protected to afford **43**. The TBS group was then removed from **43** to produce **44**. The diol was then protected via acetonidization to afford **45**. This compound was combined with **46** to afford the polyketide fragment of the analog of lagunamide B (**47**).

The synthesis of the analog of lagunamide B laid the framework for the synthesis of the target molecule, lagunamide B, and supported the conclusion that the stereocenter on C39 of

lagunamide A was misassigned. With knowledge of the misassigned stereocenter in lagunamides A and B, a total synthesis of lagunamide C is necessary to completely and confidently confirm the stereochemistry of three stereogenic centers within the polyketide fragment of the compound.



(i)  $\text{TiCl}_4$ , DIPEA, 1-NMP, DCM,  $0^\circ\text{C}$ , 88%; (ii) TBSOTf, 2,6-lutidine, DCM,  $0^\circ\text{C}$ , 93%; (iii)  $\text{LiBH}_4$ , THF/MeOH,  $0^\circ\text{C}$ , 88%; (iv)  $\text{pySO}_3$ ,  $\text{Et}_3\text{N}$ , DMSO/DCM,  $0^\circ$  to  $-78^\circ\text{C}$ , 93%; (v)  $\text{Bu}_2\text{BOTf}$ , DIPEA, DCM,  $0^\circ\text{C}$ , 63%; (vi)  $\text{LiBH}_4$ , THF/MeOH,  $0^\circ\text{C}$ , 82%; (vii) PivCl, py, DCM, 63%; (viii) HF py, THF 76%; (ix) 2,2-DMP, CSA, DCM, 81% (x)  $\text{LiCl}$ , DIPEA, ACN, 34%

**Scheme 8** Synthetic route of polyketide 47 in 15.1 adapted from Pal and Chakraborty.<sup>28</sup>

As mentioned previously, the polypeptide backbones of lagunamides A, B and C are structurally alike, and therefore, can be synthesized similarly.<sup>29</sup> The polyketide fragment of lagunamide C is unique, and will require its own synthetic route. Components of the syntheses of

the polyketide fragments within lagunamides A and B may be employed. It is proposed that eight diastereomers of the polyketide fragment within lagunamide C (**48-55**), be produced to elucidate its structure correctly, as shown in **Figure 8**.

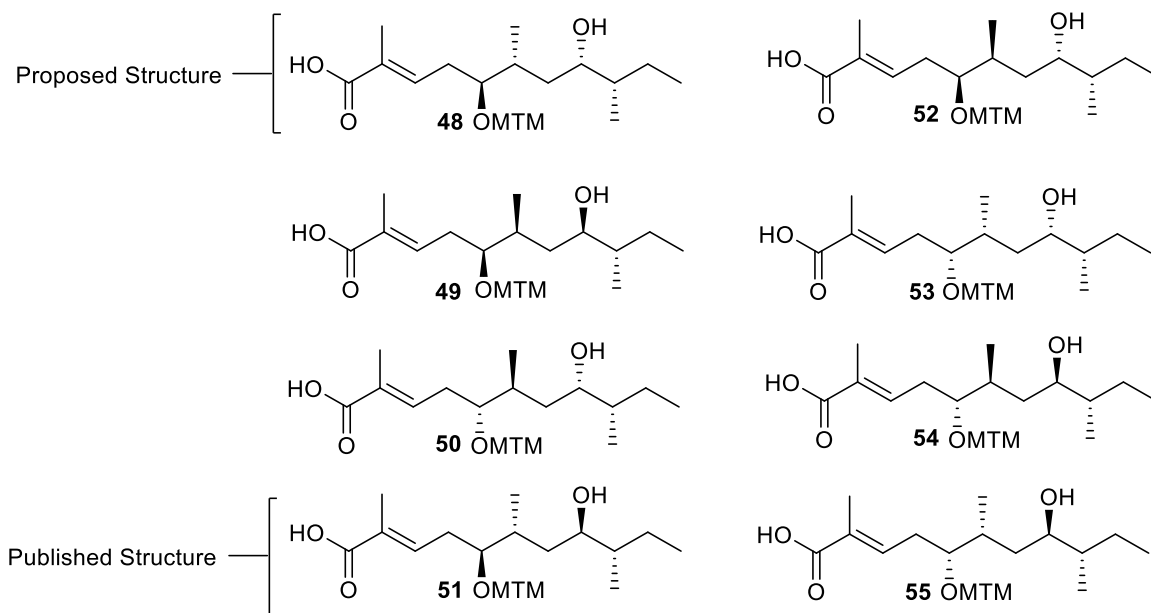
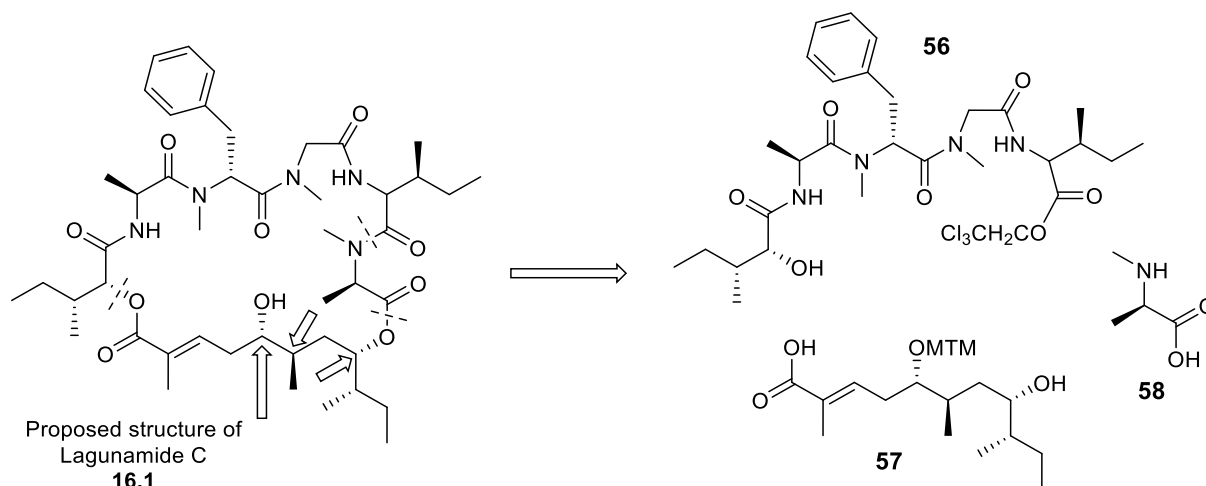


**Figure 8** Diastereomers of lagunamide C polyketide

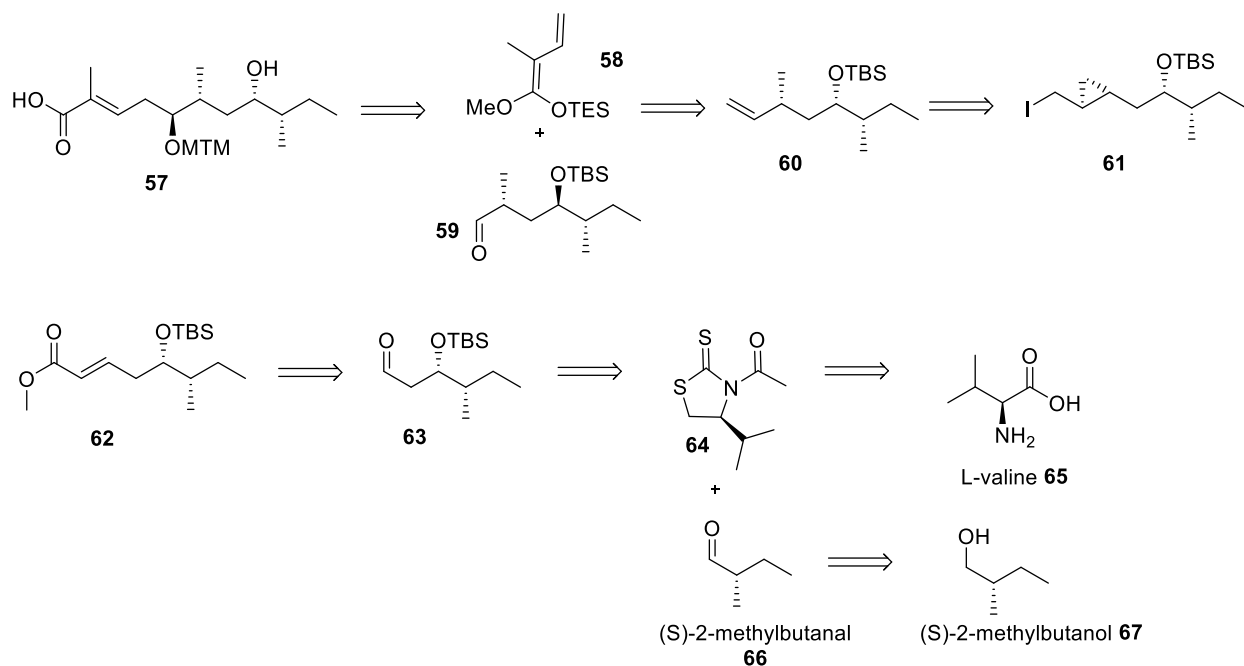
## 2.1 Retrosynthetic Analysis of Lagunamide C

The retrosynthetic analysis of the proposed structure of lagunamide C (**16.1**) breaks this natural product into three separate components: a pentapeptide backbone (**56**) a polyketide fragment (**57**) and commercially available methyl-D-alanine (**58**) as shown in **Scheme 9**. The pentapeptide backbone is composed of D-isoleucine, L-alanine, methyl-D-phenylalanine, and methyl glycine and can be constructed through a series of peptide couplings and deprotections. The retrosynthetic analysis of polyketide **57** is more intricate, as it contains three stereogenic centers and will require facially selective reactions to achieve the desired stereogenic centers.



**Scheme 9** Lagunamide C deconstruction

As shown in **Scheme 10**, compound **2** can be accessed via a Mukaiyama vinylous aldol reaction from a silyl ketene **58** and aldehyde **59**. The aldehyde can be obtained via a reductive opening of iododimethylcyclopropane **61**, which can then be accessed from **60** via its reduction to form an allylic alcohol. The allylic alcohol can then undergo a selective cyclopropanation and an iodine substitution to form **61**. Compound **62** can be accessed via Wittig olefination of **63** and compound **63** can be accessed via mixed aldol reaction of **64** and (*S*)-2-methyl butanal (**66**). Auxiliary **64** can ultimately be formed from L-valine (**65**) and (*S*)-2-methyl butanal (**66**) can be obtained via oxidation of commercially available (*S*)-2-methyl butanol (**67**).<sup>30</sup>



*Scheme 10 Retrosynthetic analysis of 57*

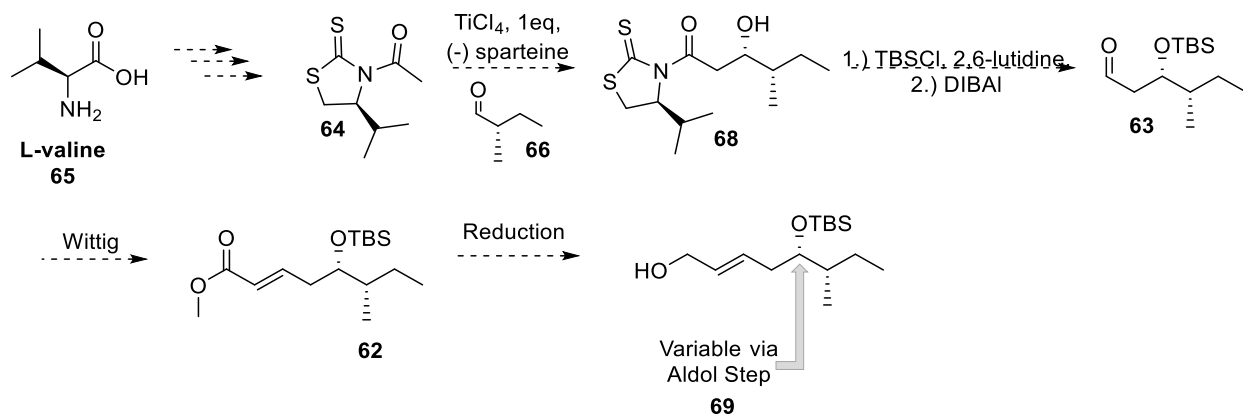
## 2.2 Proposed Work of the Polyketide Fragment

The synthesis of the polyketide of lagunamide C is organized into three modules. This modular approach allows for optimization and stereospecificity. Each module produces one of the three desired stereocenters in the polyketide, allowing access to all eight diastereomers of lagunamide C. Key steps of the proposed synthetic route include a titanium mediated mixed aldol, enantioselective cyclopropanation, Charette cyclopropane ring-opening, and CBS reduction.<sup>32, 36</sup>

### 2.2.1 Module I

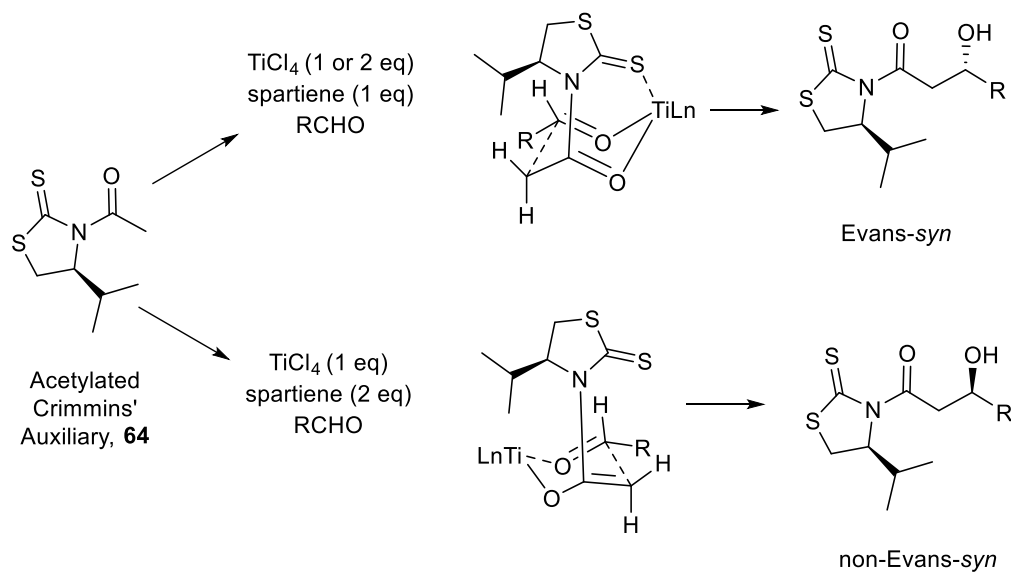
The first module of the synthesis involves forming the Crimmin's auxiliary according to methods described by Crimmins followed by the acetylation of the auxiliary.<sup>30</sup> The acetylated auxiliary (**64**) is then subjected towards a facially selective titanium mediated mixed aldol reaction as shown in the proposed route in **Scheme 11**.<sup>30, 31</sup>

**Module I: Aldol**



**Scheme 11** Module I: Forming the first stereocenter via titanium-mediated mixed aldol

In addition to the Crimmin's auxiliary, equivalent control of the titanium tetrachloride will allow for stereospecificity of the reaction. The titanium tetrachloride interacts with the thione of the thiozolidinone ring of the auxiliary, the desired aldehyde, and acetyl group on the acetylated auxiliary. The (–)-sparteine will allow for the desired chelation effect between the acetylated Crimmins and the titanium tetrachloride, thereby forming the anticipated Evans-syn product, as described by Crimmins and as shown in **Scheme 12**.<sup>30, 31</sup>

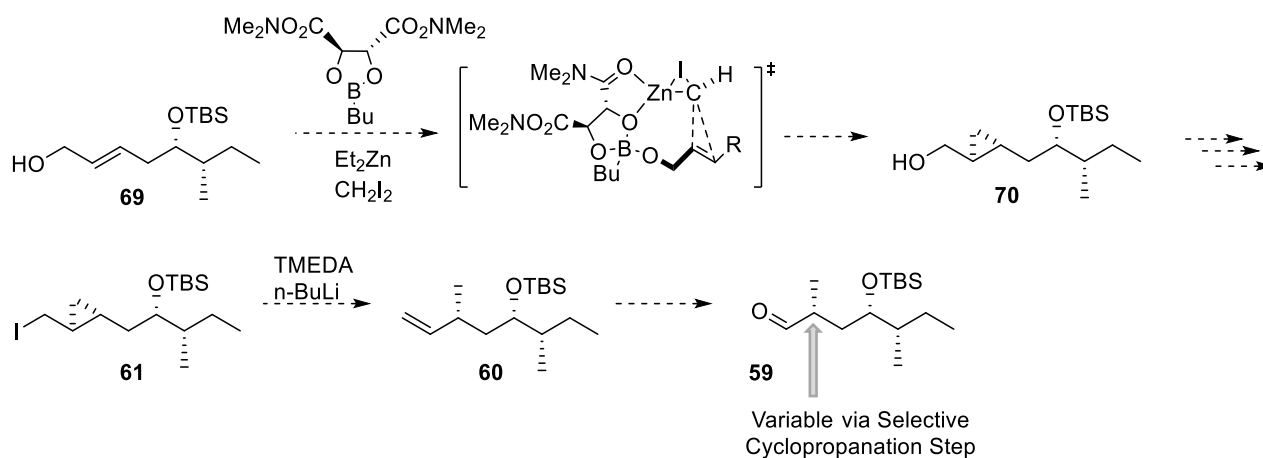


**Scheme 12** Equivalent control of  $\text{TiCl}_4$ , adapted from Hodge and Olivio and Crimmins<sup>30, 31</sup>

## 2.2.2 Module II

The second module, shown in **Scheme 13**, will begin with a Charetté cyclopropanation of the allylic alcohol produced in Module I. Facial selectivity is achieved by using (*S*)-(-)-2-methyl-CBS-oxazaborolidine, diethyl zinc, and methylene iodide.<sup>32</sup> The cyclopropanated material then will undergo a halogen exchange, followed by a ring opening olefination.<sup>32</sup> The remaining terminal olefin will then be hydroxylated and oxidized to form the aldehyde, completing module II.<sup>32, 33</sup>

### Module II: Cyclopropanation

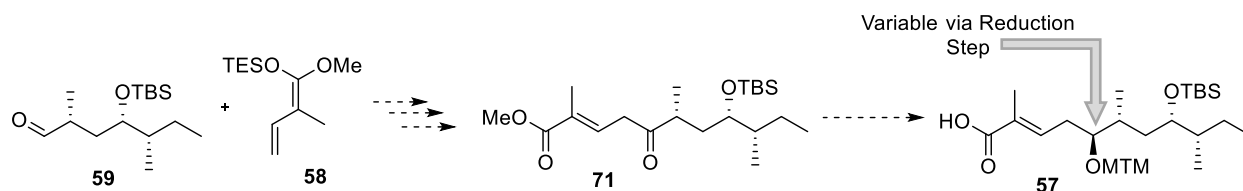


*Scheme 13* Module II: Stereospecific cyclopropanation via dioxaborolane catalysis<sup>32</sup>

## 2.2.3 Module III

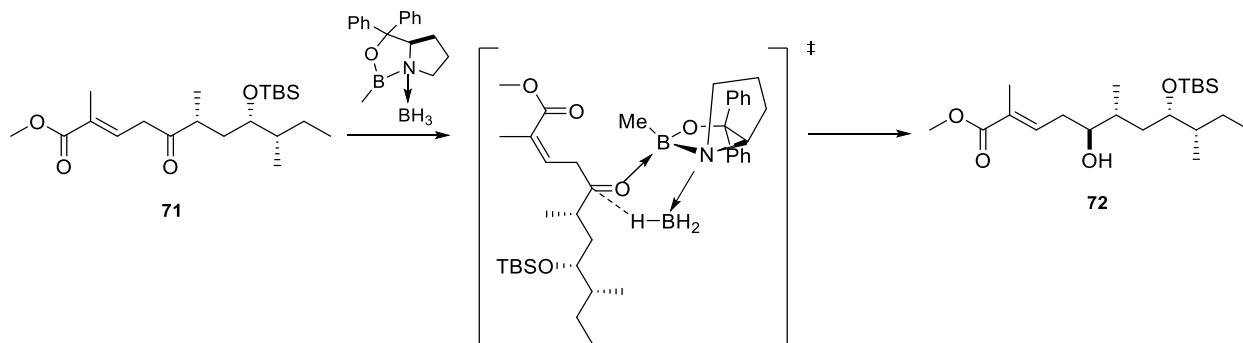
The aldehyde accessed from Module II will be subjected to a Mukaiyama aldol reaction and then to a stereoselective reduction, as illustrated in **Scheme 14**.<sup>33</sup> The proposed Mukaiyama aldol reaction has been reported to produce single diastereomers; however, it is expected that the produced diastereomer would be in the opposite configuration.<sup>33</sup> This selectivity is due to the interactions between the  $\alpha$ -methyl- $\beta$ -OTBS ketones. It is also proposed that the silylated alcohol group plays a significant role in the selectivity.<sup>33, 34, 35</sup>

### Module III: Selective Reduction



**Scheme 14** Module III: Stereoselective reduction to achieve the third stereocenter

Due to the desired stereoselectivity and the positioning of the protected hydroxyl group, an achiral reducing agent, such as  $\text{NaBH}_4$ , is insufficient for the reduction.<sup>36</sup> An enantioselective reduction technique developed by Corey that employs the catalyst, (*S*)-(-)-2-methyl-CBS-oxazaborolidine, is used to access the proposed transition state as illustrated in **Scheme 15**.<sup>36</sup> It is a useful strategy to achieve the desired conformation due to the interactions between the ketone and methylated boron, as this would allow the hydride to be added to the *si* face of the carbonyl.<sup>36</sup> The reduction of the ketone will produce the third stereocenter within the fragment, completing the polyketide fragment of lagunamide C.



**Scheme 15** Proposed transition state of CBS reduction as adapted from Corey and Halal.<sup>36</sup>

## 2.3 Summary

Previous work involving the total synthesis of lagunamide A and the total synthesis of an analog of lagunamide B have been discussed. Due to the incorrectly assigned stereocenters within lagunamides A and B, it is possible that the current assigned stereocenters within lagunamide C

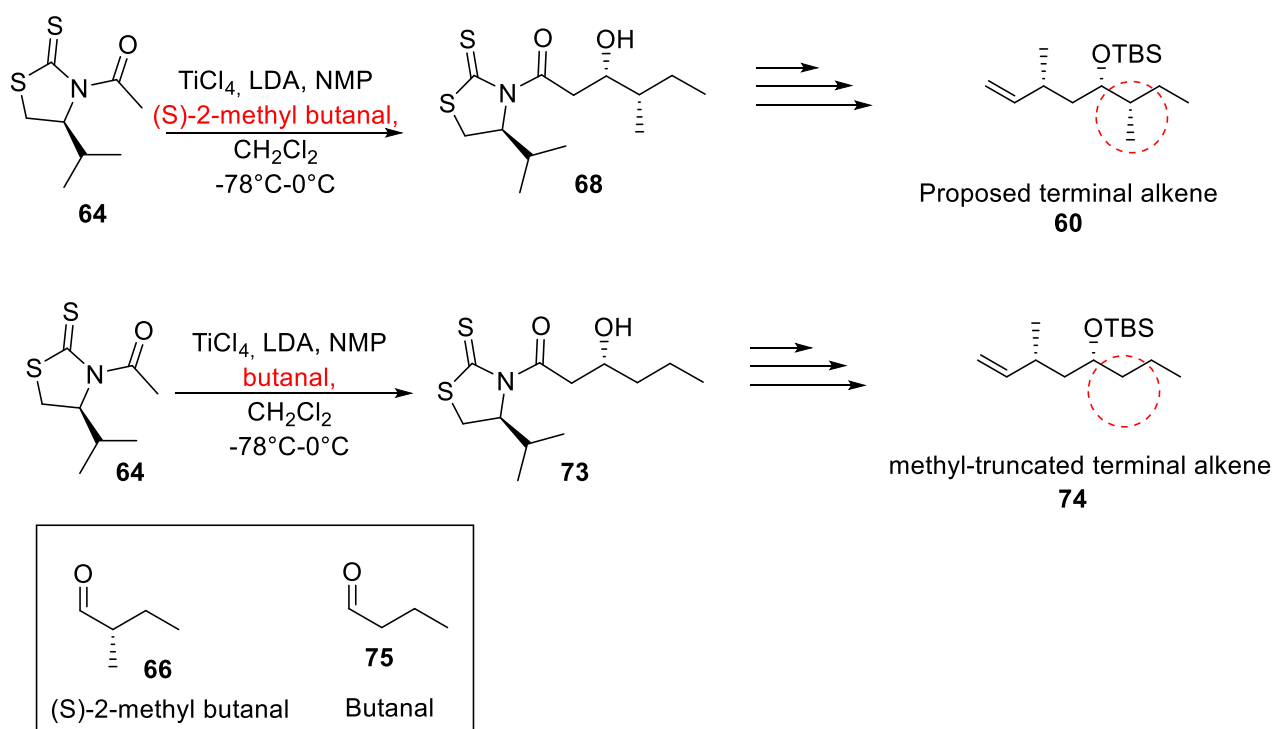


may also be incorrect. The synthetic methods used to obtain the polyketide fragments of lagunamides A and B are ineffective for synthesizing lagunamide C due to the addition of one carbon atom in the polyketide fragment of lagunamide C. This and the stereochemical inaccuracies prove that a new synthetic route is necessary to confidently confirm the structure of lagunamide C. A synthetic route that allows for the formation of all eight possible diastereomers has been proposed via a modular approach. Each module contains a key component in which a stereogenic center is formed and can be easily manipulated to achieve the desired stereochemistry.

## Chapter 3: Current Synthetic Work

### 3.1 Introduction

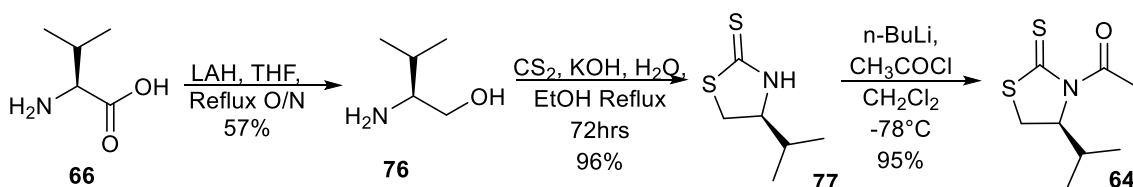
It is envisioned that the proposed modular approach for the synthesis of lagunamide C will afford a stereogenic center in each separate module. This route was tested on a model system in which butanal (**75**) was used in place of (2*S*)-2-methyl butanal (**66**) in the first module, as shown in **Scheme 16**, to produce a methyl-truncated analog of the desired system.<sup>37</sup> This model system appropriately tests the validity of the proposed route, specifically in the second module where the cyclopropanation and ring opening result in the formation of the second stereocenter. This methyl-truncated model system has thus far proven to be suitable, as the cyclopropanation and ring opening were successful.



**Scheme 16** Proposed terminal alkene vs methyl-truncated terminal alkene

## 3.2 Module I

The first module is centered on the titanium-mediated mixed aldol reaction that results in the formation of a stereogenic center. This component employs a chiral auxiliary to influence the desired stereochemical outcome. The synthesis of the Crimmins' Auxiliary is shown in **Scheme 17**. The amino acid, L-valine (**66**), was subjected towards a  $\text{LiAlH}_4$  reduction to provide L-valinol (**76**). L-Valinol (**76**) was then formed into the Crimmins auxiliary (**77**) via Crimmin's protocol in which two equivalents of carbon disulfide are used to ensure the formation of the thiazolidinethione ring instead of the oxazolidinone ring. Auxiliaries are useful because they provide facial selectivity and can be removed with relative ease.<sup>31</sup>

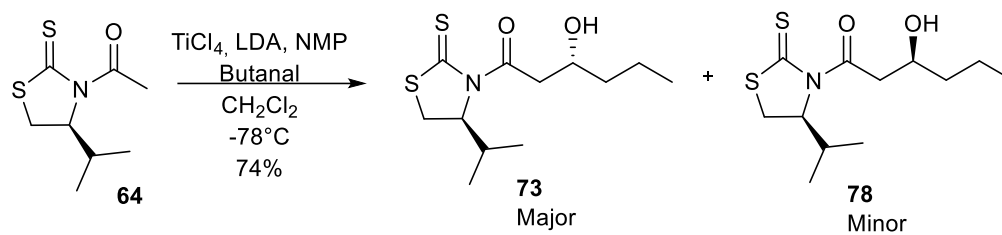


**Scheme 17** Formation and acetylation of Crimmins' Auxiliary

A thiazolidinethione ring was selected for the synthesis due to the reduced nucleophilicity of the thione versus a ketone in the subsequent mixed aldol reaction.<sup>31</sup> Thione auxiliaries are also more easily removed and recovered than oxazolidinone rings.<sup>30, 31</sup> This, in addition to equivalent control, allows for favorable interactions with the base, titanium, and aldehyde during the mixed aldol reaction that leads to the desired conformation of the products, as discussed in the proposed route.<sup>31</sup>

Following the formation of the auxiliary, it was acetylated to form **64** and subjected towards a titanium-mediated mixed aldol reaction and formed two separable diastereomers (**73**, **78**). While the proposed route suggests using (-)-sparteine as a chiral base, NMP and LDA provided the same effect and produced the desired product at comparable yields through equivalent control

of the titanium tetrachloride and the chelation effect of the NMP and LDA. 29 Zhou and coworkers used a very similar procedure to obtain diastereomers **73** and **78** as was used in this work. The difference is the Zhou group's use of a non-chiral base, DIPEA, in place of the LDA and NMP combination employed here.<sup>37</sup> This difference may account for the stereochemical inversion observed with the formed products.



**Scheme 18** Titanium-mediated mixed aldol reaction

The stereochemistry of **73** and **78** were confirmed by comparing the spectra to identified compounds by Zhou and coworkers.<sup>37</sup> The <sup>1</sup>H-NMR data was characterized for both diastereomers produced by the reaction, but there was uncertainty about the stereochemistry of each compound. Suggestions were made due to the interactions resulting from the equivalent control of the TiCl<sub>4</sub> in the mixed aldol reaction, the relative polarity of the compounds, and the amounts of each compound produced. It was hypothesized that the major diastereomer contained the *R* configuration. These questions were validated by comparing the spectra of the compound formed by Zhou and coworkers. There are distinctive peaks in the 3.5-3.2 range, highlighted in gray in **Table 1**, that indicate the similarities between the two synthesized compounds.<sup>37</sup> The spectra of

**73** is illustrated in **Figure 9**. Diastereomer **73** was used for the remainder of the synthesis after identifying its configuration.<sup>37</sup>

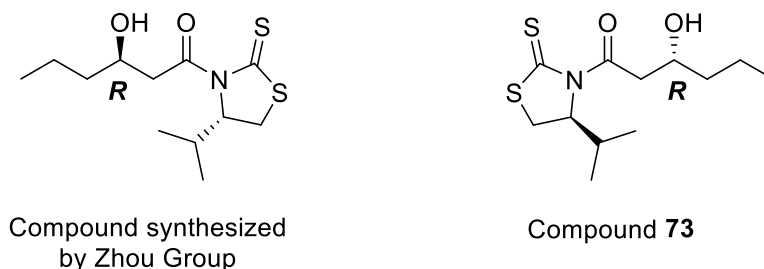


**Figure 9** Compound synthesized by Zhou Group vs. Compound **73**

No.	<sup>1</sup> H-NMR ppm- Zhou	<sup>1</sup> H-NMR ppm- Compound <b>73</b>
5	5.17 (ddd, 1H, J = 7.61, 6.42, 1.01 Hz, H-9)	5.18 (ddd, J = 7.6, 6.2, 1.2 Hz, 1H),
13	4.03 (m, 1H, H-4)	4.03 (m, J = 8.5, 7.4 Hz, 1H),
11,4	3.51 (dd, 1H, J = 11.6, 7.98 Hz, H-8)	3.55 – 3.41 (m, 2H)
	3.43 (dd, 1H, J = 17.4, 9.35 Hz, H-5)	
4	3.32 (dd, 1H, J = 17.4, 2.65 Hz, H-5)	3.34 (m, J = 2.8 Hz, 1H)
11	3.03 (dd, 1H, J = 11.6, 1.10 Hz, H-8)	3.04 (d, J = 11.5, 1.2 Hz, 1H)
6	2.35 (ABX6, 1H, J = 6.78 Hz, H-10)	2.42 – 2.29 (m, J = 7.0 Hz, 1H)
14,15	1.58 - 1.33 (m, 4H, H-2, H-3)	1.64 – 1.32 (m, 4H)
7,8,16	1.05 (d, 3H, J = 6.88 Hz, H-11)	1.09 – 1.04 (d, 3H)
	0.98 (d, 3H, J = 6.77 Hz, H-11)	0.98 (d, J = 6.9 Hz, 3H)
	0.92 (t, 3H, J = 6.97 Hz, H-1)	0.95 – 0.90 (m, 3H).

**Table 1** Proton NMR Comparison of **73**<sup>37</sup>

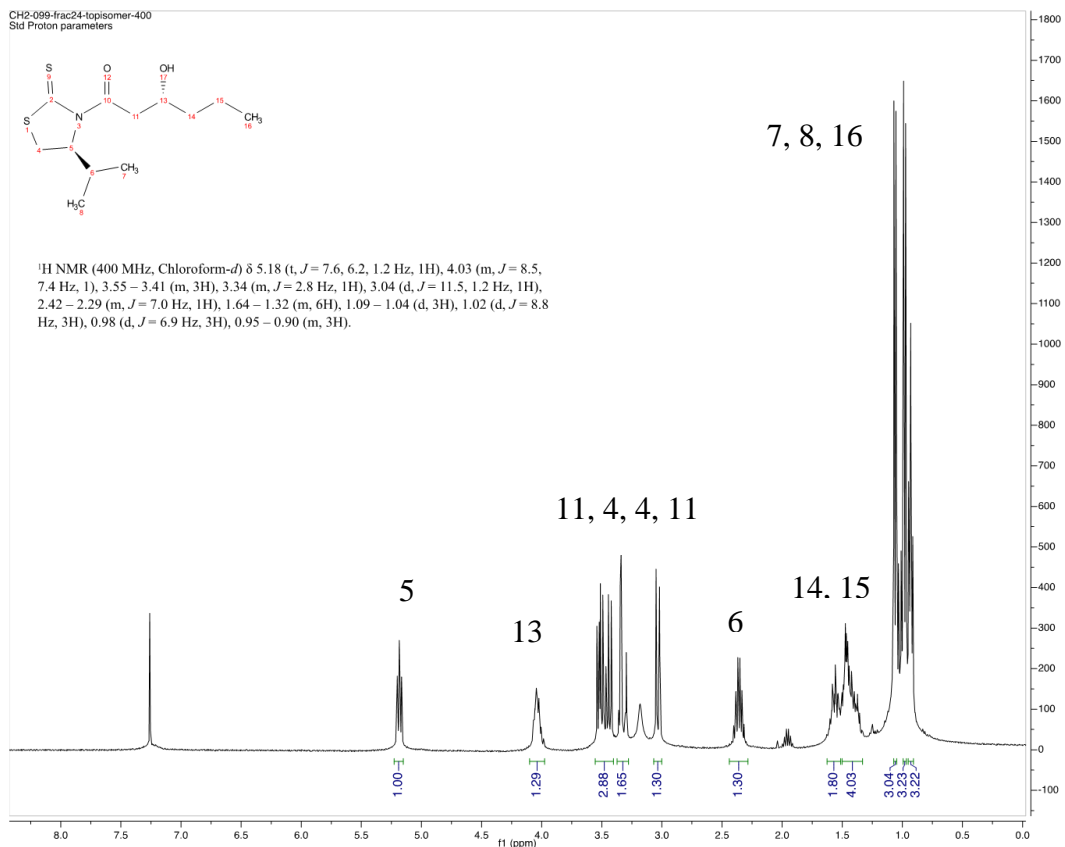
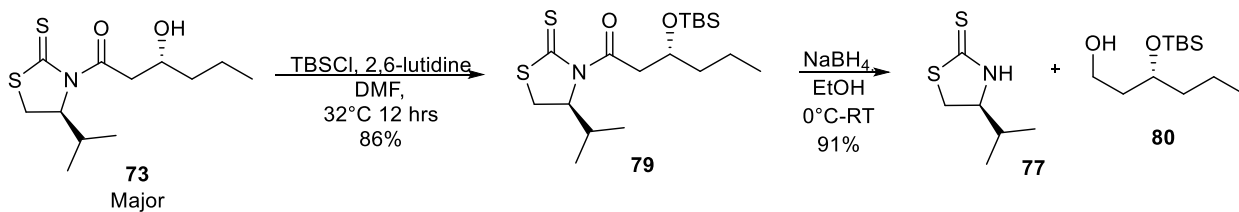


**Figure 10** Proton NMR of **73**

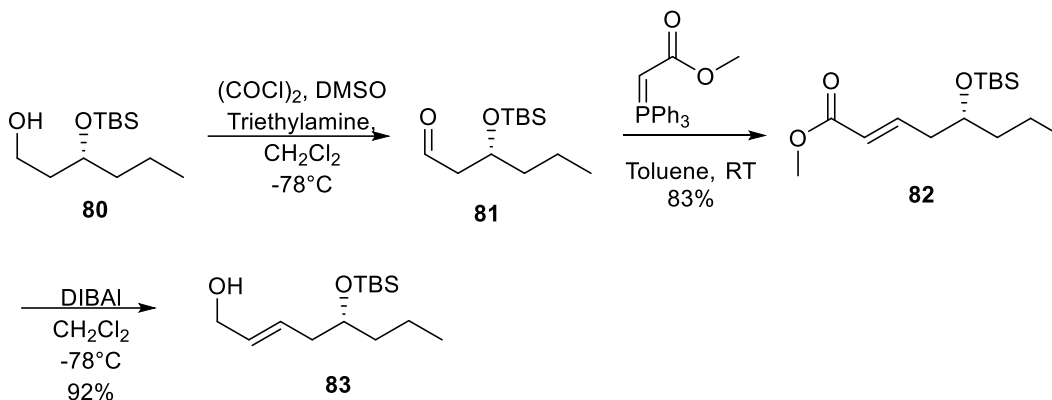
Following the isolation of **73**, it was TBS protected to give **79** and underwent reductive cleavage of the auxiliary to reveal primary alcohol **80** via NaBH<sub>4</sub> reduction, as shown in **Scheme 19**.



**Scheme 19** TBS protection and reductive cleavage of **73**

The remaining alcohol (**80**) was then oxidized via Swern oxidation to aldehyde **81**. With **81** in hand, it was subjected towards a Wittig olefination to afford ester **82**. The ester (**82**) was then

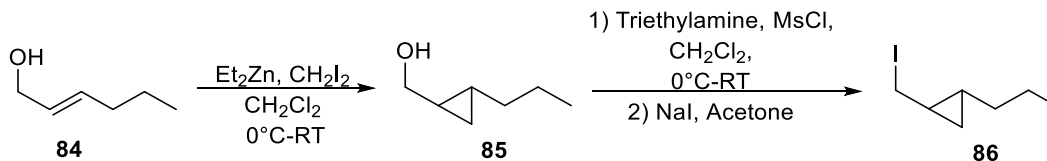
reduced via DIBAL-H reduction to afford allylic alcohol **83**. The production of alcohol **83** successfully completed Module I of the synthetic route, as shown in **Scheme 20**.



**Scheme 20** Oxidation, Wittig olefination, DIBAL-H reduction

### 3.3 Module II

Before beginning the second module with **83**, a model system using trans-2-hexenol (**84**) was initially used to confirm the effectiveness of the cyclopropanation, mesylation, and halogenation, as shown in **Scheme 21**.



**Scheme 21** Model system of cyclopropanation and halogenation using 2-hexenol (**84**)

Several approaches were attempted before achieving a successful cyclopropanation. These approaches included various temperature conditions and reaction times, as outlined in **Table 2**. It was originally proposed to perform this step via facially selective dioxaborolane catalyst, but was completed under non-stereospecific conditions in an attempt to prove the success of the cyclopropanation and conserve the dioxaborolane catalyst.<sup>36, 37</sup> The cyclopropanation proved to be

effective, but did not provide separable diastereomers in neither the trans-2-hexenol model system nor methyl truncated system.

Reagents	Temperature Conditions	Outcome
CH <sub>2</sub> I <sub>2</sub> , ZnEt <sub>2</sub> , TiCl <sub>4</sub>	0 °C to -20 °C, stir 7 hours at -20 °C	SM decomposition
	0 °C to -20 °C stir 7 hours at -20 °C in cold room	SM decomposition
ZnEt <sub>2</sub> , CH <sub>2</sub> I <sub>2</sub>	-20 °C stir 7 hours in cold room	Partial cyclopropanation
	0 °C to RT, stir O/N	Product, 95 % yield

**Table 2** Reaction conditions of cyclopropanation of **84**

After the successful cyclopropanation of **84**, the mixture of cyclopropanated material (**85**) was then subjected towards mesylation of the primary alcohol, followed by the iodine-substitution (**86**), illustrated previously in **Scheme 21**. Several methods were attempted to ensure the desired mesylation and halogenation products were formed. These attempts involved various temperature conditions, reaction times, and order of reactant addition as outlined in **Table 3**. It was ultimately found that the mesylated material quickly degraded after being formed and that direct halogenation of the crude mesylated material was necessary to achieve the desired iodine-substituted product.

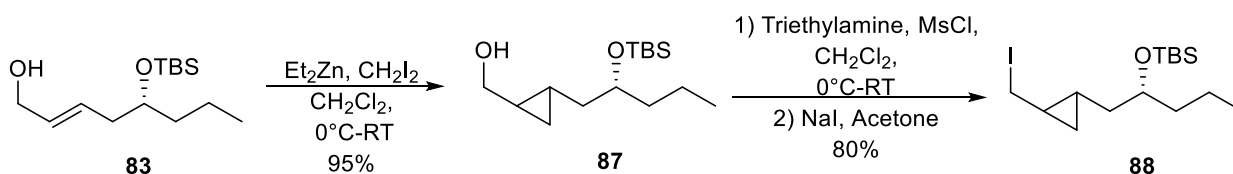
Reagents	Reaction Conditions	Outcome
1.) MsCl, triethylamine in DCM 2.) NaI in acetone	1.) 0 °C 2.) RT	Low yields <10%
	Allowed NaI to stir O/N before workup and purification	SM decomposition
1.) MsCl, triethylamine, THF 2.) NaI, THF	1.) 0°C 2.) RT	Low yields <10%
	Allowed NaI to stir O/N before workup and purification	SM decomposition
1.) MsCl, triethylamine, DCM 2.) NaI in acetone	Completed full workup before subjecting towards second reaction	SM decomposition
	Completed full workup and purification before subjecting towards second reaction	SM decomposition
	Allowed NaI to stir O/N before workup and purification	SM decomposition



Table 3 Continued		
Reagents	Reaction Conditions	Outcome
1.) MsCl, triethylamine, DCM 2.) NaI in acetone	Removed DCM after stirring for approximately 45 minutes at 0 °C before subjecting to second reaction	Low yields <10%
1.) Triethylamine, MsCl, DCM 2.) NaI in acetone	Changed order of addition in mesylation, 0 °C, DCM removed after approximately 45 min., continued immediately with second reaction	Worked, higher yields >60%, Selected as appropriate procedure

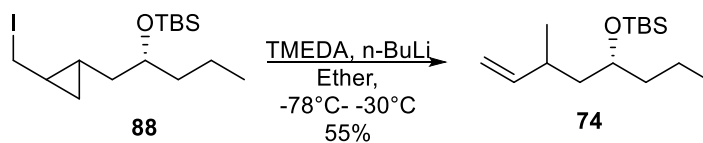
**Table 3** Halogenation reaction conditions completed with **85**

Once the model system had proven to be successful, these methods were applied to the desired system and successfully resulted in the iodine-substituted cyclopropanated material, **88**, as shown in **Scheme 22**.



**Scheme 22** Cyclopropanation, iodine substitution of **83**

The iodine-substituted compound (**88**) then underwent lithium-halogen exchange, followed by a Charett cyclopropane ring-opening, to afford the desired terminal alkene **74** in 55% yield. This step produced two separable diastereomers and is shown in **Scheme 23**. The successful formation of terminal alkene **74** shows that the proposed route is effective and can be applied towards the synthesis of lagunamide C.



**Scheme 23** Charett ring-opening of **88**<sup>32</sup>

### 3.4 Summary

Module I and the key steps of module II have been successfully completed with a methyl-truncated system. The truncated system was employed in order to more rapidly and economically test the suggested route of obtaining the polyketide fragment. The truncated system also allowed for the formation of possible analogs to be subjected towards future cytotoxicity screenings. While the chiral base (-)-sparteine was substituted for NMP and LDA during the titanium-mediated mixed aldol reaction, separable diastereomers were produced to afford the first stereogenic center within the polyketide fragment. The configurations of the diastereomers were confirmed and the desired configuration was continued in the synthetic route.

The key steps of module II, the cyclopropanation and ring opening, were initially tested using a model system with trans-2-hexenol. Once the reaction conditions using the model system were optimized successfully via non-facially selective methods, they were applied towards the desired system to produce the terminal alkene. The cyclopropanation produced two diastereomers that were later separated following the Charette ring-opening reaction. The ring opening of the cyclopropane reveals the second stereogenic center of the polyketide, thereby accessing two of the three questionable stereogenic centers within the polyketide fragment. Completing these key steps validates the current synthetic route and can be applied towards the target system to synthesize lagunamide C.

## Chapter 4: Conclusion and future work

### 4.1 Conclusion

Total synthesis is a relatively economic and ecological method of obtaining biologically active compounds derived from natural products when compared to extraction.<sup>1, 20</sup> This method has been applied to obtain a plethora of drugs used to treat a multitude of conditions including various types of cancer, pain, strabismus, and hyperactive sweating.<sup>8, 9, 14, 16, 23</sup> Many of these fascinating compounds are derived from secondary metabolites and often used by organisms as defense mechanisms.<sup>6, 24, 26</sup> While terrestrial sources have produced many useful natural products, the earth's oceans are also an invaluable source for new synthetically interesting and bioactive compounds.<sup>22, 23, 26, 29</sup>

The bioactive compound lagunamide C has yet to be synthesized. There is dispute towards the assignment of three stereocenters within the polyketide portion of the compound. A selective, modular approach has been proposed to synthesize the polyketide fragment within this compound and confidently assign the unknown stereocenters. This approach has first been applied towards a methyl-truncated analog of lagunamide C, which will lay the foundation for the synthesis of the polyketide fragment of lagunamide C and potential future analogs.

The final stages of achieving a scalable, synthetic pathway for a methyl truncated analog of lagunamide C are underway by using the proposed modular approach. The current synthetic route has proven to be scalable. The synthetic route suggested the use of chiral catalysts to achieve the ideal stereochemistry of the compounds. Non-selective methods have been used initially to ensure the formation of the product and have been useful for possible analog studies. It has also been found that the diastereomers produced in the non-selective steps are separable via column chromatography.

The stereochemistry has been confirmed for the stereogenic center produced in Module 1 by comparing spectral data to previously synthesized compounds.<sup>37</sup> The key components of the proposed route, the cyclopropanation and Charette cyclopropane ring-opening have been effective, thus validating the proposed route. These techniques will be later applied towards synthesizing lagunamide C.

## **4.2 Future work**

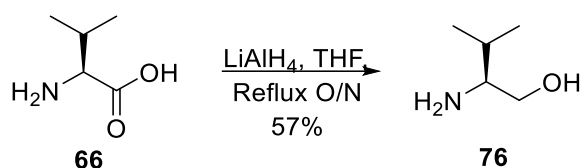
Future work will include applying this established synthetic route to accomplish the total synthesis of the of lagunamide C. Components of the current synthetic route may be altered to achieve higher selectivity at the titanium-mediated mixed aldol stage, as the current methods allow for some selectivity. This could be adjusted to produce the desired stereocenter at higher yields by using a more sterically hindering auxiliary to influence the stereo-selectivity in the reaction or using (-)-sparteine as suggested in the proposed route.

In Module II, a dioxaborolane catalyst is suggested to promote stereoselectivity towards the cyclopropanation; however, the diastereomers are separable following the ring-opening of the cyclopropane ring.<sup>32</sup> For the purpose of producing analogs, it may be favorable to consider not using the catalyst and move forward with the synthetic route with the separated compounds. Following the completion of Module II, the route will be applied towards the synthesis of lagunamide C. The synthesis of the pentapeptide backbone is currently underway and will be joined with the prepared polyketide fragment once synthesis of the fragment is completed.

## Chapter 5: Experimental Procedures

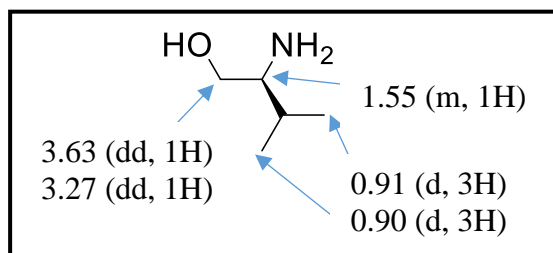
**Experimental Details:** Reactions completed with anhydrous protocol were completed in flame-dried glassware under argon. Dry solvents were obtained directly from a solvent system. All products were dried with anhydrous sodium sulfate as part of the workup. Compounds were purified via flash-silica chromatography with specified solvent systems, unless otherwise noted.  $^1\text{H-NMR}$  and  $^{13}\text{C-NMR}$  data were obtained from a Varian 400 MHz at Kansas State University. High-resolution mass spectra were obtained using a LCT Premier Time of Flight mass spectrometer at the University of Kansas.

### L-Valinol



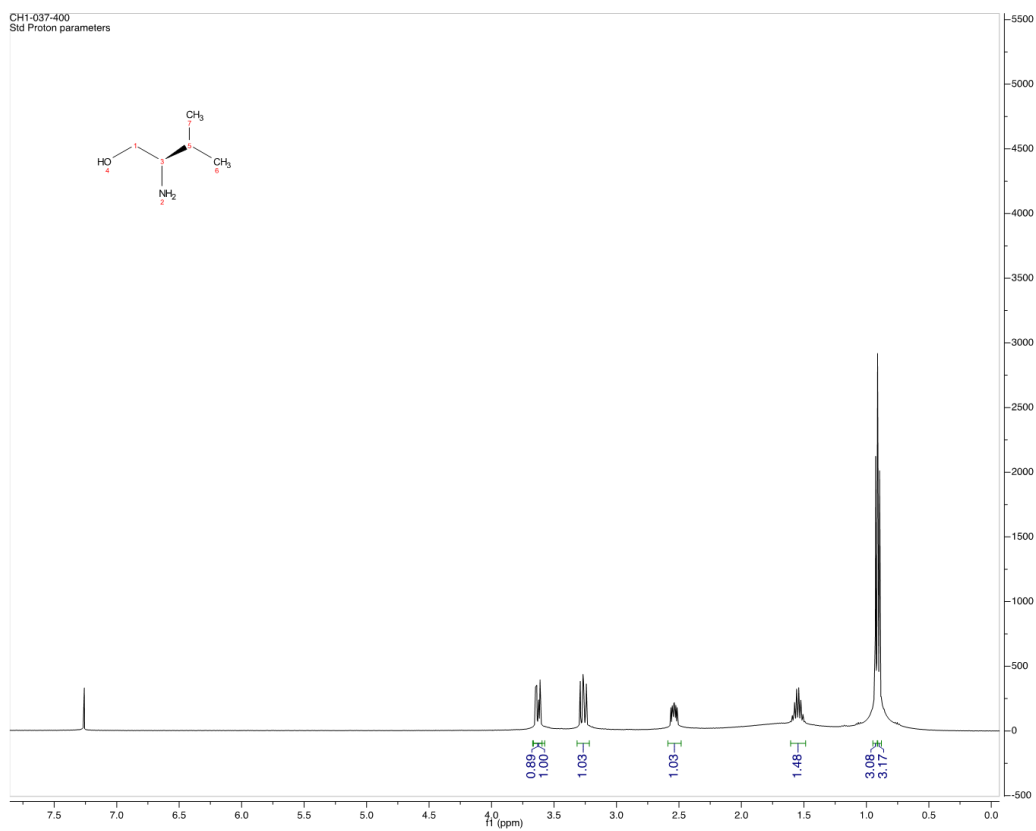
In a dry, round bottom flask,  $\text{LiAlH}_4$  (1.88g, 51 mmol, 3 eq.) and THF (0.24 M) were combined and cooled to 0 °C. L-valine, **66**, (2.00g, 17 mmol, 1 eq.) was added slowly while stirring. The ice bath was removed and the mixture was warmed to room temperature. The solution was then refluxed overnight at 70 °C. The solution was diluted with ether and cooled to 0 °C. The  $\text{LiAlH}_4$  was quenched with  $\text{H}_2\text{O}$  and 15%  $\text{NaOH}$ , forming a white precipitate. The solution was decanted into another flask and the precipitate was rinsed with ether. The liquid was added to the solution and the white precipitate was disposed. Alternatively, saturated Rochelle salt solution can be added to the flask and stirred overnight. The aqueous layer can then be extracted with  $\text{CH}_2\text{Cl}_2$  (x3), and the resulting organic layers dried and concentrated to afford an oily, crude product. The crude product was purified via short path vacuum distillation resulting in obtaining **76** (1.00 g, 57 %).

## Key $^1\text{H-NMR}$ Peaks of L-Valinol

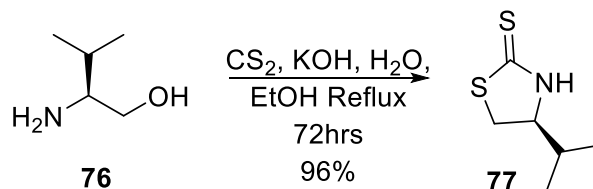


**$^1\text{H-NMR}$  (400 MHz, Chloroform-d):**  $\delta$  3.63 (dd,  $J = 10.4, 4.0$  Hz, 1H), 3.27 (dd,  $J = 10.4, 8.9$  Hz, 1H), 2.54 (m,  $J = 8.9, 6.4, 4.0$  Hz, 1H), 1.54 (m,  $J = 13.5, 6.7$  Hz, 1H), 0.92 (d,  $J = 6.1$  Hz, 3H), 0.90 (d,  $J = 6.1$  Hz, 3H).

**Notebook: CH1-045**

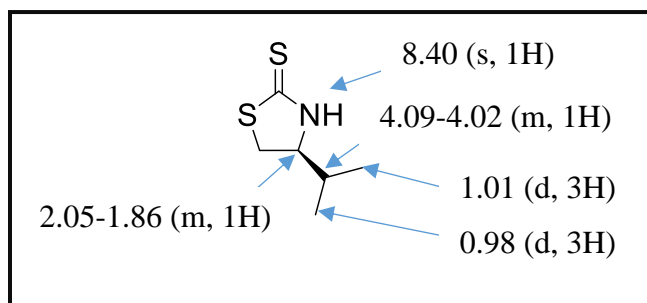


### (S)-4-isopropylthiazolidine-2-thione



L-valinol, **76**, (10.00 g, 96.7 mmol, 1 eq.),  $\text{CS}_2$  (15.2 mL, 251.8 mmol, 2.6 eq.), and EtOH (29.3 mL, 3.3 M) were combined in a round bottom flask. An addition funnel was attached to the flask, flushed with argon, and charged with 2.25M KOH (116.3 mL, 261.6 mmol, 2.25 M). The KOH was slowly added to the flask with stirring. After the KOH was added, the addition funnel was replaced with a condensing tube and flushed with argon. The solution was left to reflux at 80 °C for 72 hours. Over the course of the reflux period, the solution changed from bright orange to light yellow. The flask was then cooled to room temperature and volatiles were removed under reduced pressure. The solution was acidified with 1 M HCl and then extracted with  $\text{CH}_2\text{Cl}_2$  (x3). The combined organic layers were then dried and concentrated under reduced pressure, producing a light yellow solid. The crude product, **77** (15.04 g, 96 %), was used for subsequent reactions without further purification

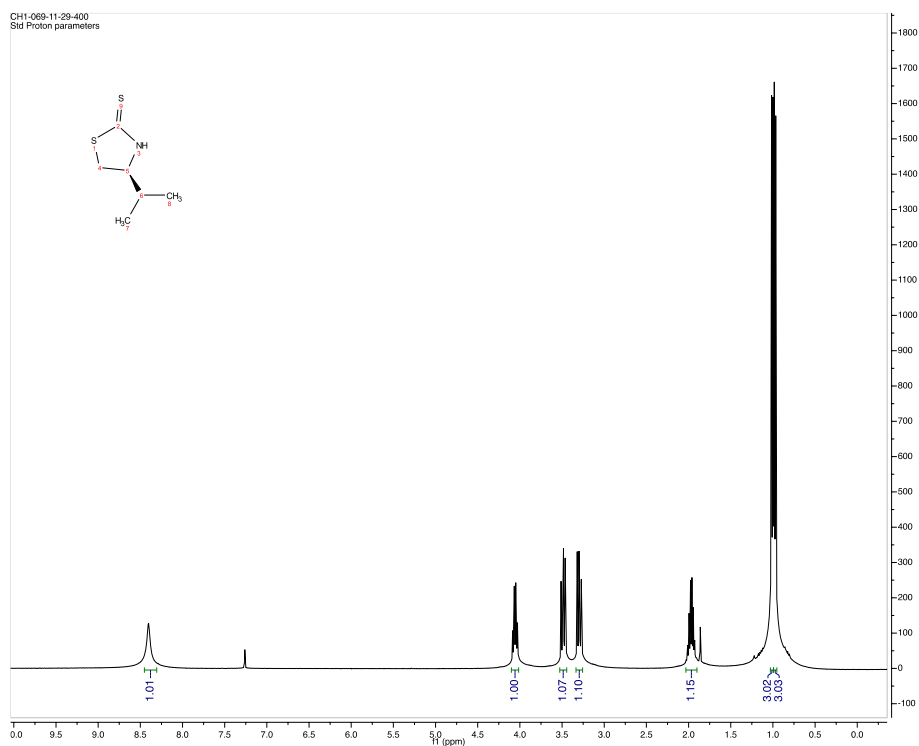
#### Key $^1\text{H-NMR}$ Peaks of (S)-4-isopropylthiazolidine-2-thione



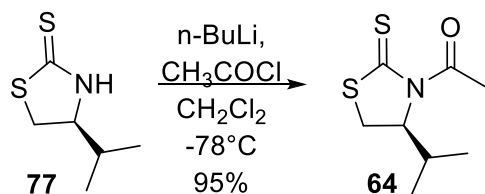
**$^1\text{H-NMR}$  (400 MHz, Chloroform-*d*):**  $\delta$  8.40 (s, 1H), 4.09 – 4.02 (q, 1H), 3.49 (dd,  $J = 11.2, 8.3$  Hz, 1H), 3.30 (dd,  $J = 11.2, 8.2$  Hz, 2H), 2.05 – 1.86 (m,  $J = 6.7$  Hz, 1H), 1.01 (d,  $J = 6.8$  Hz, 3H), 0.98 (d,  $J = 6.8$  Hz, 3H).

**HRMS:** calculated for  $[C_6H_{11}NS_2 + H^+]$  162.0406, found 162.0402.

**Notebook:** CH1-401



**(S)-1-(4-isopropyl-2-thioxothiazolidin-3-yl)ethan-1-one**

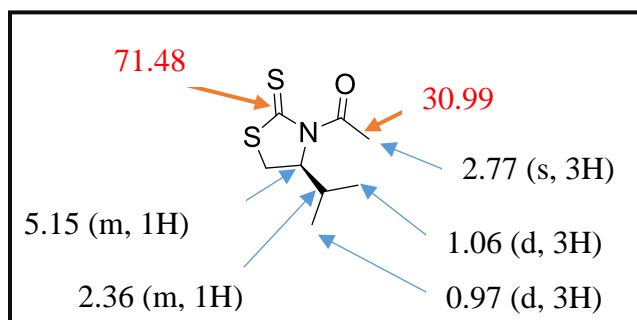


A dry round bottom flask was charged with crude **77** (2.00 g, 12.4 mmol, 1 eq.) and dry THF (8.26 mL, 1.5 M). The solution was cooled to  $-83^\circ\text{C}$  via ethyl acetate-dry ice bath and then 1.6 M n-BuLi (8.53 mL, 13.64 mmol, 1.1 eq.) was added dropwise. A color changed of light yellow, to orange, to bright yellow was observed throughout the addition of the n-BuLi. Approximately 20 minutes later, acetyl chloride (1.15 mL, 16.12 mmol, 1.3 eq.) was added dropwise and 20 minutes afterward, the solution was warmed to room temperature. The reaction



was quenched with NH<sub>4</sub>Cl saturated solution and water, extracted with CH<sub>2</sub>Cl<sub>2</sub> (x3), dried, and concentrated under reduced pressure. Flash silica chromatography (2:1 CH<sub>2</sub>Cl<sub>2</sub>/ Hexane) afforded **64** (2.40 g, 95%).

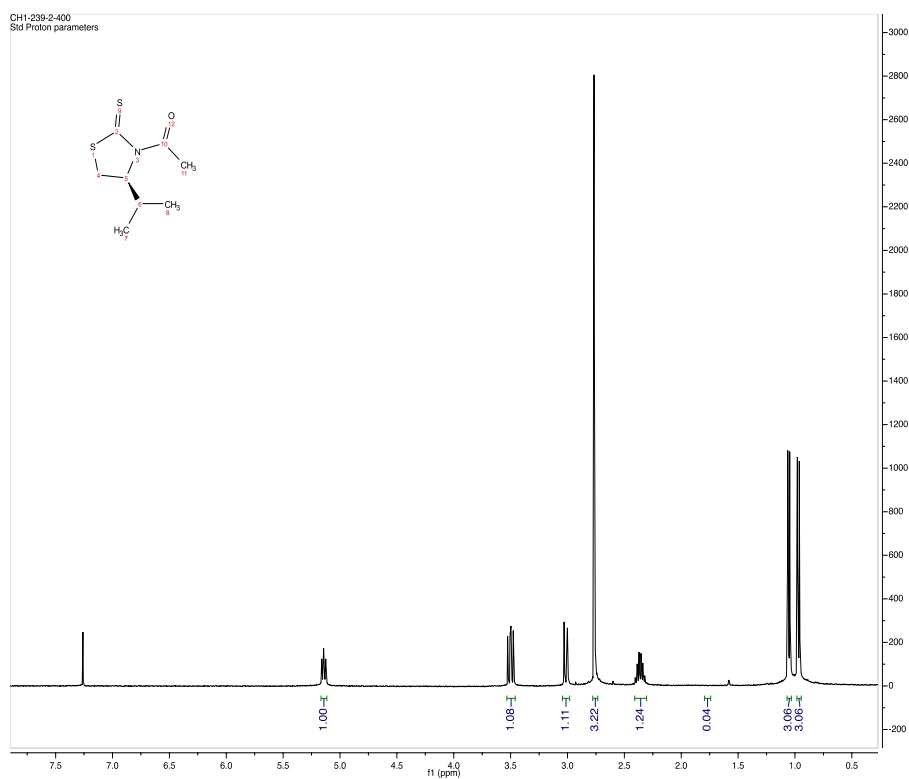
Key <sup>1</sup>H-NMR and <sup>13</sup>C-NMR Peaks of (S)-1-(4-isopropyl-2-thioxothiazolidin-3-yl)ethan-1-one

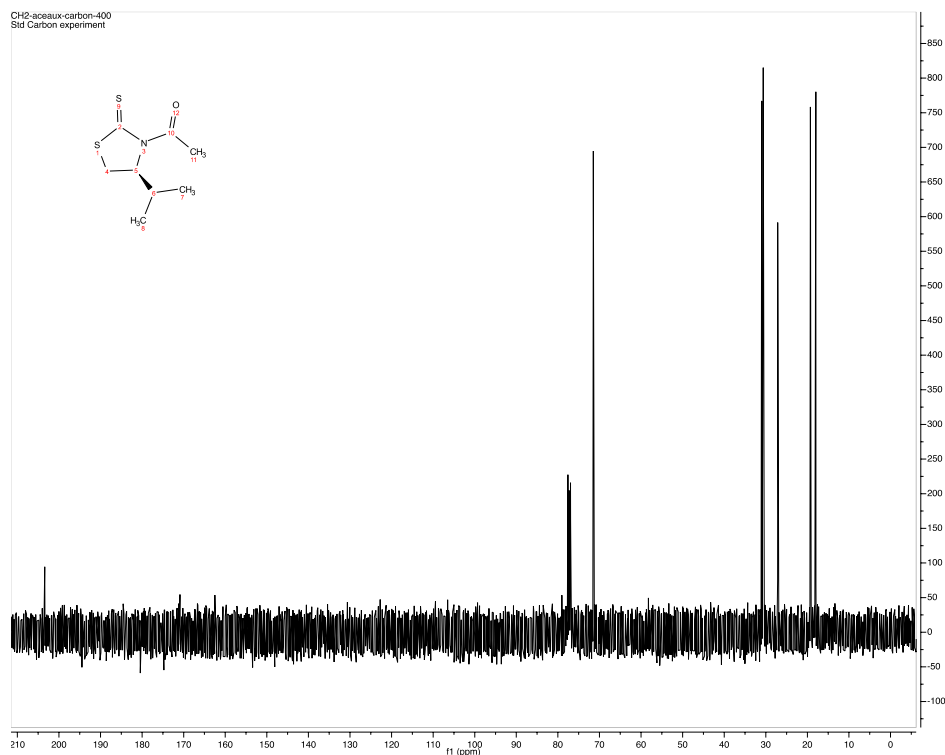


<sup>1</sup>H-NMR (400 MHz, Chloroform-*d*):  $\delta$  5.14 (m,  $J = 7.6, 6.2, 1.2$  Hz, 1H), 3.50 (dd,  $J = 11.5, 8.0$  Hz, 1H), 3.02 (dd  $J = 11.5, 1.2$  Hz, 1H), 2.77 (s, 3H), 2.36 (m,  $J = 13.4, 6.8$  Hz, 1H), 1.06 (d,  $J = 6.8$  Hz, 3H), 0.97 (d,  $J = 6.9$  Hz, 3H).

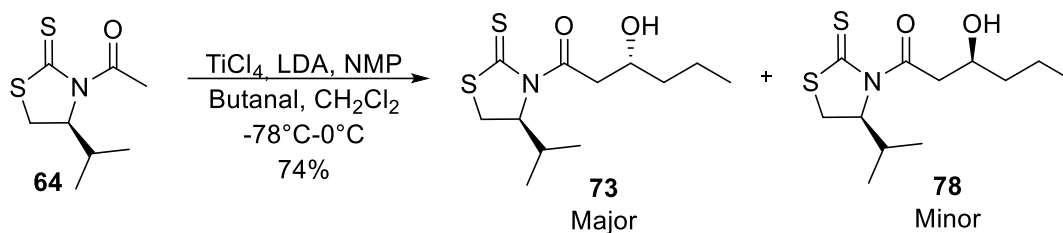
<sup>13</sup>C-NMR (101 MHz, Chloroform-*d*):  $\delta$  203.42, 71.48, 30.99, 30.63, 27.14, 19.27, 17.97.

Notebook: CH1-239





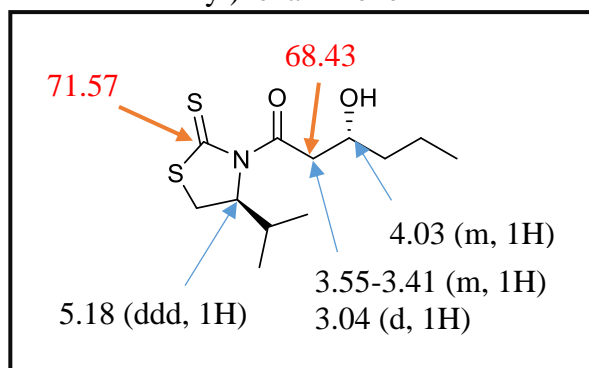
**(R)-3-hydroxy-1-((S)-4-isopropyl-2-thioxothiazolidin-3-yl)hexan-1-one**



A dry round bottom flask was charged with **64** (1.06 g, 5.21 mmol, 1 eq.) and  $\text{CH}_2\text{Cl}_2$  (10.42 mL, 0.5 M). The contents were cooled to  $0^\circ\text{C}$ .  $\text{TiCl}_4$  (0.60 mL, 5.47 mmol, 1.05 eq.) was added dropwise, changing the solution from a bright yellow to a bright orange color. Meanwhile, 0.62 M LDA was prepared by adding 2.58 mL of diisopropylamine in 18.0 mL of THF and adding 11.88 mL n-BuLi (1.6 M in hexanes) at  $-78^\circ\text{C}$ . Approximately 20 minutes after adding the  $\text{TiCl}_4$ , the freshly prepared 0.62 M LDA (10.10 mL, 6.25 mmol, 1.2 eq.) was added to the solution, changing the color from bright orange into a deep burgundy. NMP (0.60 mL, 6.25 mmol, 1.2 eq.) was added approximately 20 minutes later. The solution was cooled to  $-78^\circ\text{C}$  and then 10 minutes

later, the butanal (0.63 mL, 7.82 mmol, 1.5 eq.) in CH<sub>2</sub>Cl<sub>2</sub> (1.45 mL, 5.4 M) was added. Thirty minutes following the addition of the aldehyde, the solution was warmed from -78 °C to 0 °C with an ice bath. It was quenched with NH<sub>4</sub>Cl, diluted with brine, and extracted with CH<sub>2</sub>Cl<sub>2</sub> (x4). The combined organic layers were then dried and concentrated under reduced pressure. Flash silica chromatography (2:1 hexanes/ ethyl acetate) afforded the product, composed of 2 diastereomers, **73** (380 mg) and **78** (238 mg) and a mixture of **73** and **78** (439 mg) with an overall yield of 74%.

Key <sup>1</sup>H-NMR and <sup>13</sup>C-NMR Peaks of (R)-3-hydroxy-1-((S)-4-isopropyl-2-thioxothiazolidin-3-yl)hexan-1-one

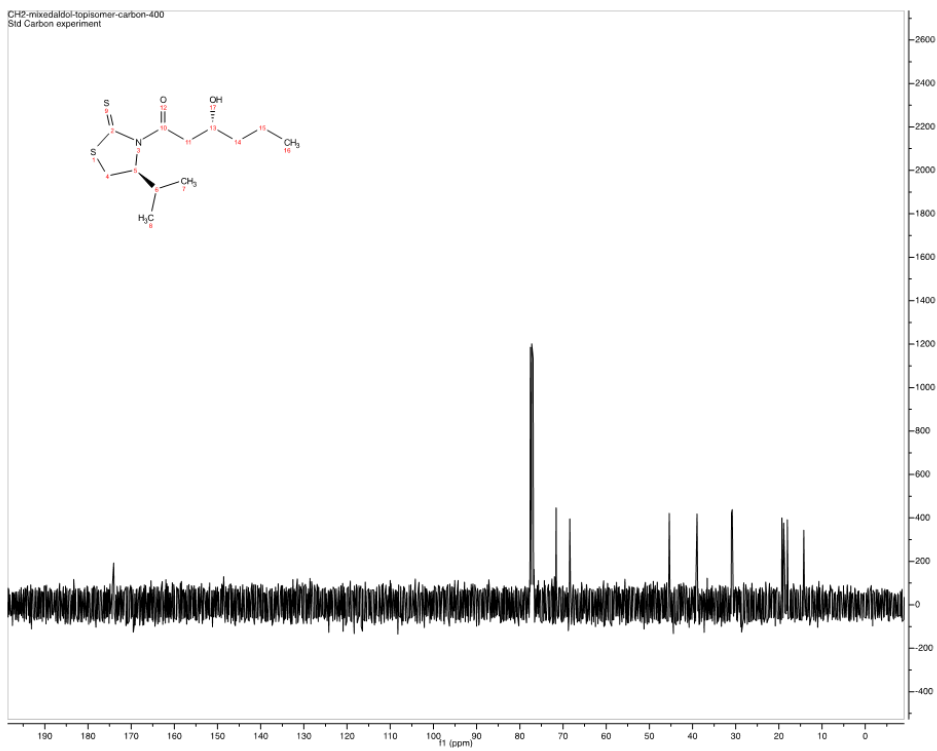
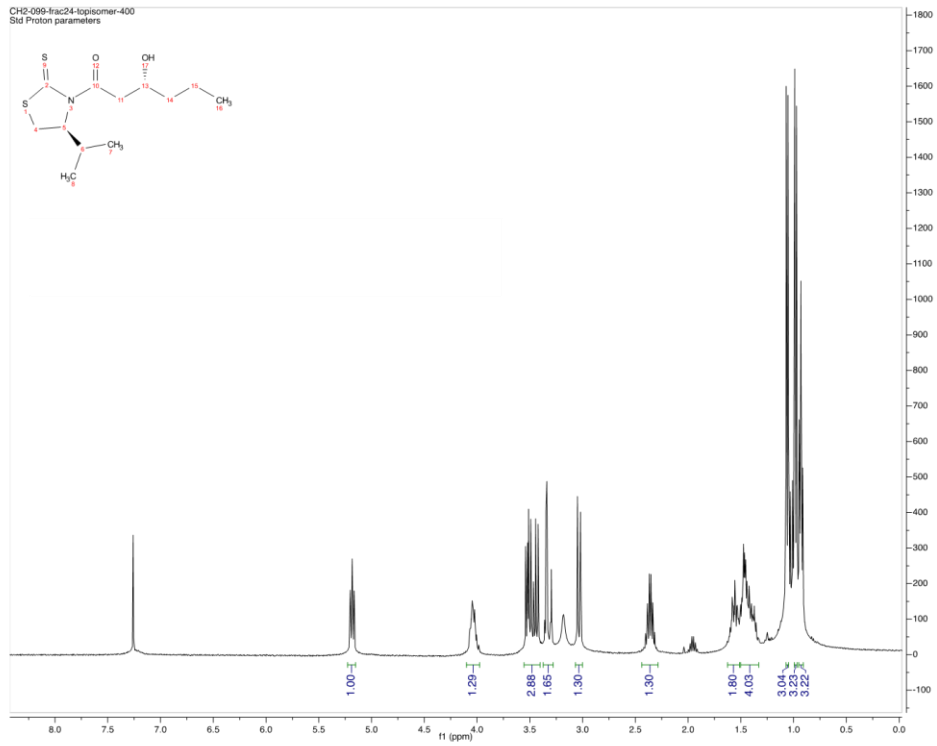


<sup>1</sup>H NMR (400 MHz, Chloroform-*d*): δ 5.18 (ddd, *J* = 7.6, 6.2, 1.2 Hz, 1H), 4.03 (m, *J* = 8.5, 7.4 Hz, 1), 3.55 – 3.41 (m, 1H), 3.34 (m, *J* = 2.8 Hz, 1H), 3.04 (d, *J* = 11.5, 1.2 Hz, 1H), 2.42 – 2.29 (m, *J* = 7.0 Hz, 1H), 1.64 – 1.32 (m, 4H), 1.09 – 1.04 (d, 3H), 0.98 (d, *J* = 6.9 Hz, 3H), 0.95 – 0.90 (d, 3H).

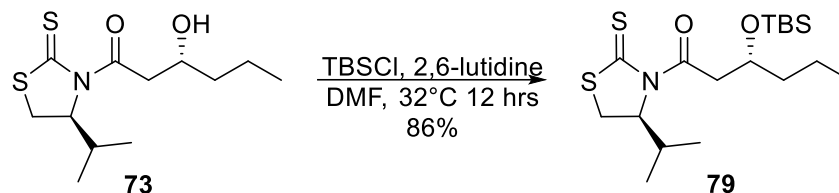
<sup>13</sup>C NMR (101 MHz, Chloroform-*d*): δ 174.03, 71.57, 68.43, 45.37, 38.97, 30.99, 30.80, 19.31, 18.90, 18.04, 14.23.

HRMS: calculated for [C<sub>12</sub>H<sub>21</sub>NS<sub>2</sub>O<sub>2</sub> + Na<sup>+</sup>] 298.0906, found 298.0907.

Notebook: CH2-070

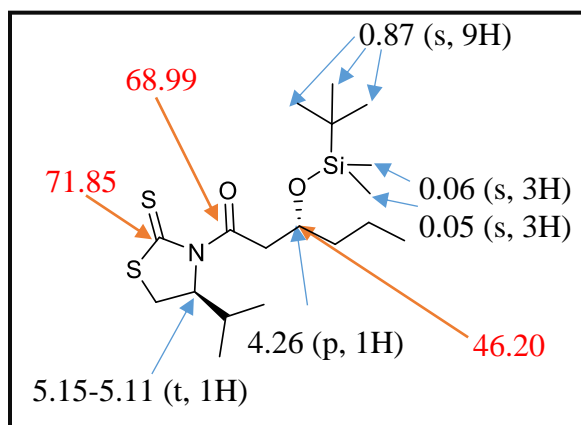


**(R)-3-((tert-butyldimethylsilyl)oxy)-1-((S)-4-isopropyl-2-thioxothiazolidin-3-yl)hexanone**



A dry round bottom flask was charged with **73** (900.0 mg, 3.27 mmol), DMF (13.6 mL, 0.24 M), TBSCl (1.97 g, 13.08 mmol, 4 eq.), and 2,6-lutidine (1.90 mL, 16.35 mmol, 5 eq.). The solution was stirred overnight at 33 °C under argon. To quench, the solution was diluted with ethyl acetate and extracted H<sub>2</sub>O (x6), brine (x1), dried, and concentrated. The crude, yellow compound was purified via flash silica chromatography (20:1 hexane/ethyl acetate) to produce **79** (1.29 g, 86 %).

Key <sup>1</sup>H-NMR and <sup>13</sup>C-NMR Peaks of  
(R)-3-((tert-butyldimethylsilyl)oxy)-1-((S)-4-isopropyl-2-thioxothiazolidin-3-yl)hexanone

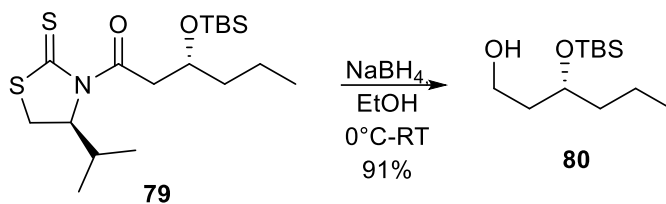


**<sup>1</sup>H NMR (400 MHz, Chloroform-*d*):**  $\delta$  5.15 – 5.11 (t, 1H), 4.26 (p,  $J$  = 5.8 Hz, 1H), 3.56 – 3.44 (m, 2H), 3.38 (dd,  $J$  = 16.8, 6.3 Hz, 1H), 3.01 (d,  $J$  = 11.5, 1.1 Hz, 1H), 2.37 (m,  $J$  = 13.5, 6.8 Hz, 1H), 1.50 – 1.41 (m, 3H), 1.36 (m,  $J$  = 15.8, 8.0, 5.8 Hz, 3H), 1.05 (d,  $J$  = 6.8 Hz, 3H), 0.97 (d,  $J$  = 6.9 Hz, 3H), 0.90 (t,  $J$  = 7.2 Hz, 3H), 0.87 (s, 9H), 0.06 (s, 3H), 0.05 (s, 3H).

**<sup>13</sup>C NMR (101 MHz, Chloroform-*d*):**  $\delta$  71.85, 68.99, 46.20, 40.11, 31.08, 30.38, 26.06, 25.92, 19.33, 18.49, 17.84, 14.45, -4.40.

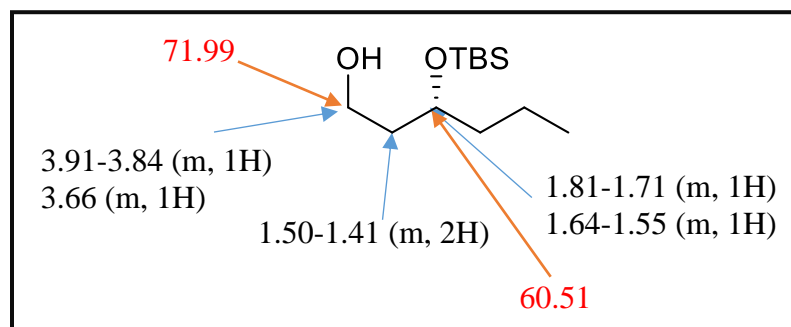


**(R)-3-((tert-butyldimethylsilyl)oxy)hexanol**



A round bottom flask was charged with **79**, (1.76 g, 4.50 mmol, 1 eq.), EtOH (26.47 mL, 0.17 M), and NaBH<sub>4</sub> (681 mg, 18 mmol, 4 eq.). The solution was stirred for approximately 4 hours. The bright yellow color of the starting material disappears as the reaction proceeds. To quench, a saturated solution of NH<sub>4</sub>Cl is added slowly to neutralize the solution. The solution is extracted with CH<sub>2</sub>Cl<sub>2</sub> (x3), brine (x1), dried, and concentrated under reduced pressure. Water may also be added during the extraction to dissolve any of the salts remaining in solution. The crude, clear oil is purified via flash silica chromatography (5:1 ethyl acetate/ hexane) to afford a clear oil, the desired alcohol, **80** (1.05 g, 91% yield), and white solid, **77** (725.76 g, 85%).

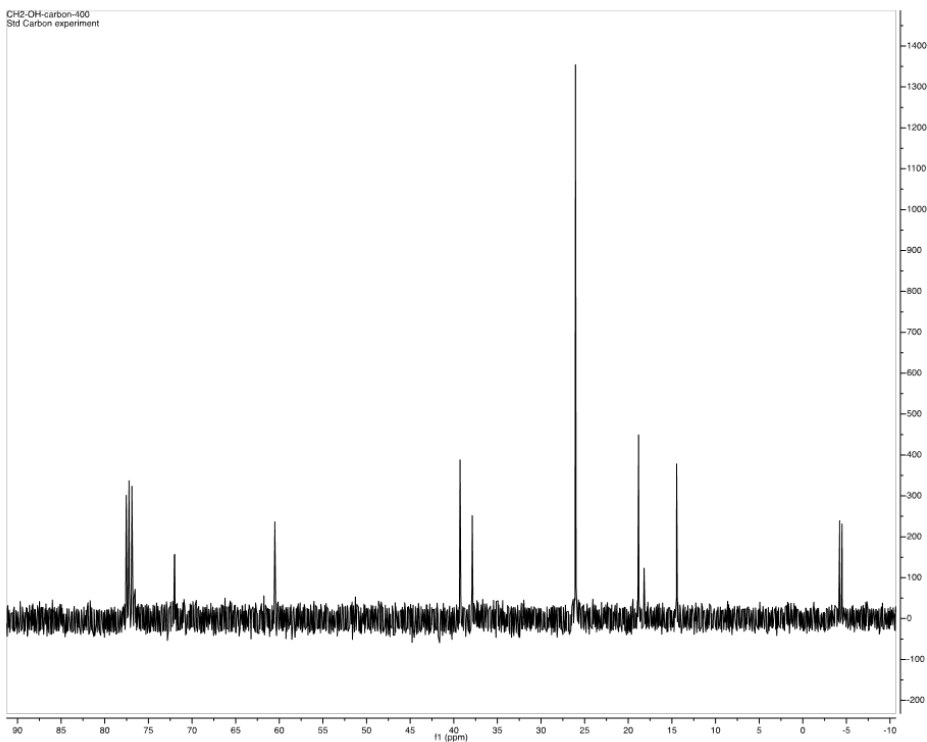
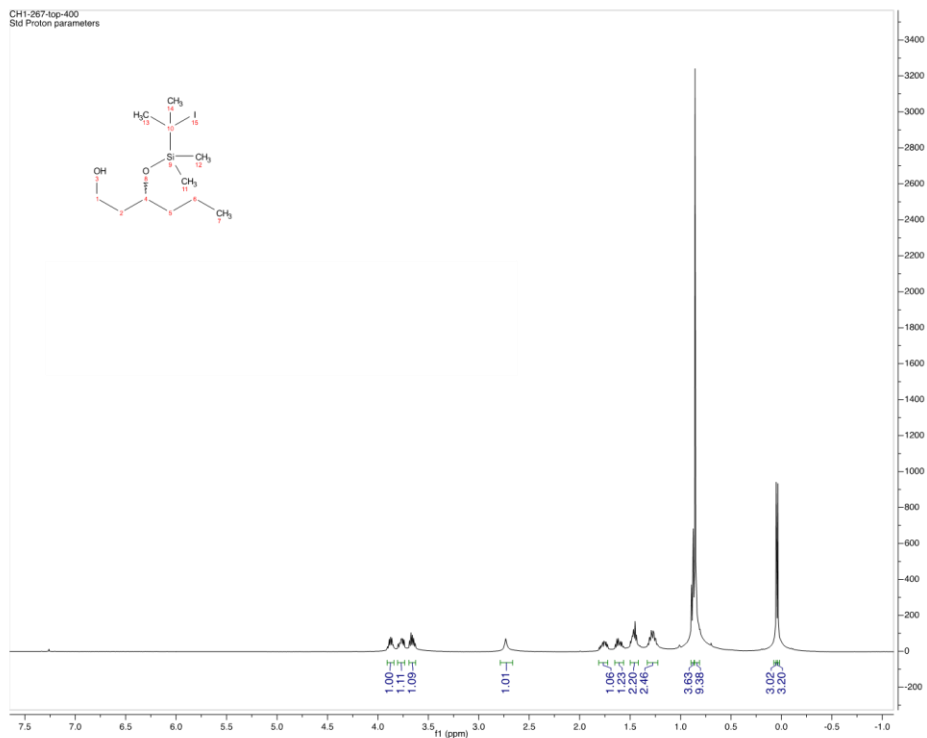
Key <sup>1</sup>H-NMR and <sup>13</sup>C-NMR Peaks for (R)-3-((tert-butyldimethylsilyl)oxy)hexanol



<sup>1</sup>H NMR (400 MHz, Chloroform-*d*): δ 3.91 – 3.84 (m, 1H), 3.77 (m, *J* = 10.7, 8.0, 4.8 Hz, 1H), 3.66 (m, *J* = 10.9, 5.5 Hz, 1H), 2.73 (s, 1H), 1.82 – 1.71 (m, 1H), 1.64 – 1.55 (m, 1H), 1.50 – 1.41 (m, 2H), 1.33 – 1.21 (m, 2H), 0.88 (t, *J* = 7.3 Hz, 9H), 0.86 (s, 3H), 0.05 (s, 3H) 0.04 (s, 3H).

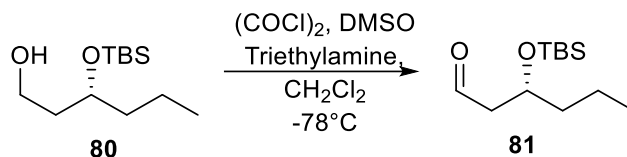
<sup>13</sup>C NMR (101 MHz, Chloroform-*d*): 71.99, 60.51, 39.29, 37.88, 26.05, 18.82, 18.19, 14.46, -4.22, -4.49.

**HRMS:** calculated for [C<sub>19</sub>H<sub>34</sub>O<sub>2</sub>Si + Na<sup>+</sup>] 345.2226, found 345.2213.  
**Notebook:** CH1-393



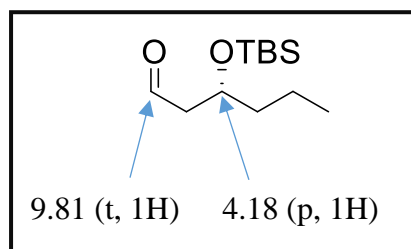


**(R)-3-((tert-butyldimethylsilyl)oxy)hexanal**



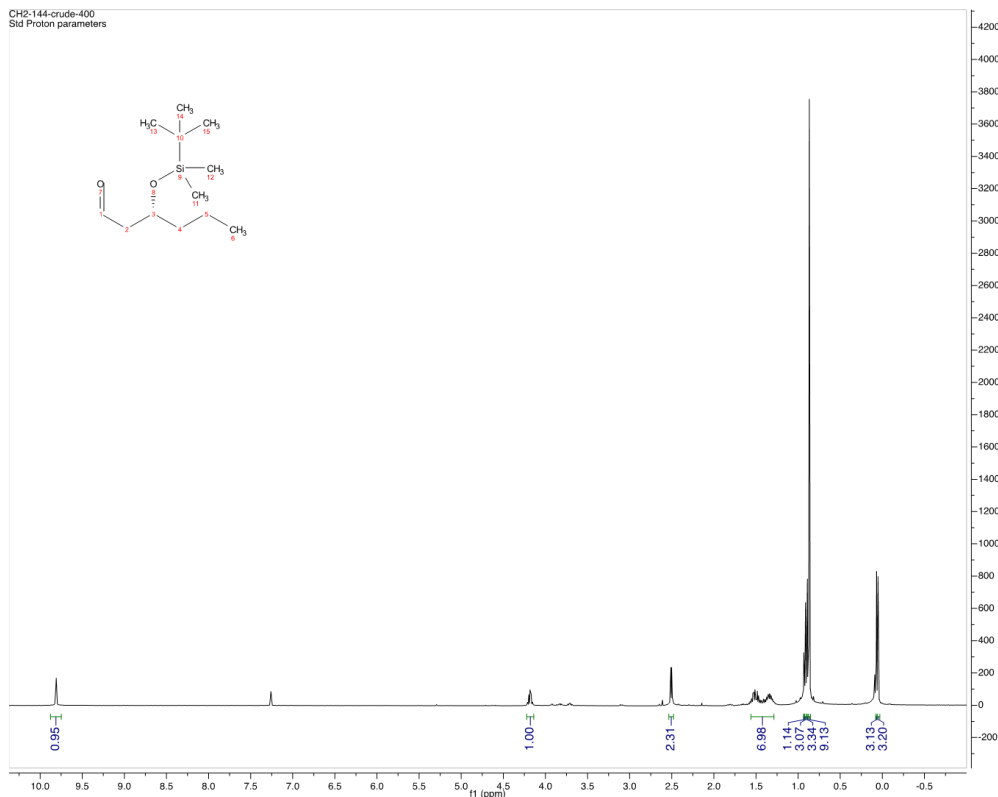
To a dry round bottom flask was added oxalyl chloride (0.25 mL, 2.83 mmol, 1 eq.) and  $\text{CH}_2\text{Cl}_2$  (5.66 mL, 0.5 M). The solution was cooled to  $-78^\circ\text{C}$ . DMSO (0.40 mL, 5.59 mmol, 2.2 eq.) was slowly added to the solution. Approximately 15 minutes later, **80** (597.5 mg, 2.57 mmol, 1 eq.) in  $\text{CH}_2\text{Cl}_2$  (2.28 mL, 1.125 M) was added and stirred. Triethylamine (1.78 mL, 12.85 mmol, 5 eq.) was added 1 hour later. The flask was then removed from the ice bath and warmed to room temperature. The solution was quenched with water and extracted with  $\text{CH}_2\text{Cl}_2$  (x3). The collected organic layers were washed once with 2% HCl solution and once with 5%  $\text{Na}_2\text{CO}_3$  solution. The organic layers were then dried and concentrated under reduced pressure. The reaction produced the crude aldehyde, **81** (1.37 g) and was used immediately for the subsequent reaction.

Key  $^1\text{H-NMR}$  Peaks for (R)-3-((tert-butyldimethylsilyl)oxy)hexanal

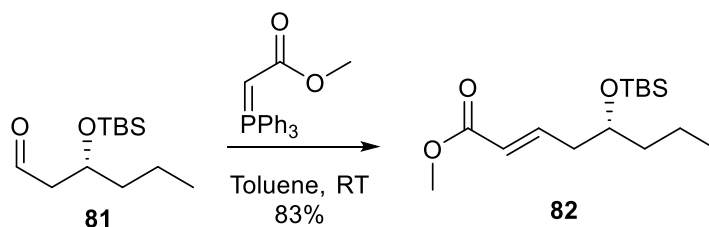


$^1\text{H NMR}$  (400 MHz, Chloroform-*d*):  $\delta$  9.81 (t,  $J = 2.5$  Hz, 1H), 4.18 (p,  $J = 5.9$  Hz, 1H), 2.51 (dd,  $J = 5.7, 2.5$  Hz, 2H), 1.58 – 1.44 (m, 3H), 1.42 – 1.26 (m, 3H), 0.94 – 0.89 (t, 3H), 0.87 (s, 9H), 0.07 (s, 3H), 0.05 (s, 3H).

**Notebook: CH2-144**

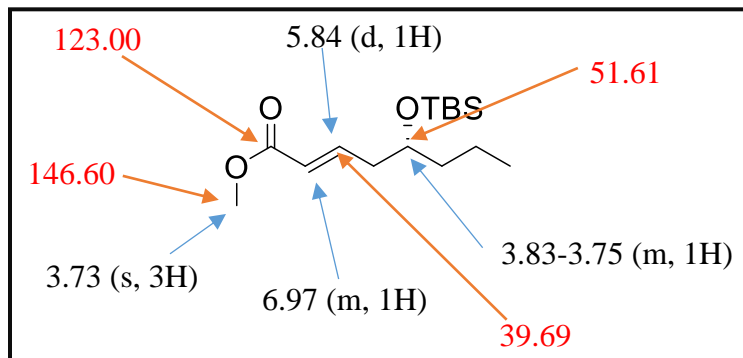


### Methyl (R,E)-5-((tert-butyldimethylsilyl)oxy)oct-2-enoate



To a dry round bottom flask was added the activated Wittig reagent (1.05 g, 3.15 mmol, 1.5 eq.) and dry toluene (6.30 mL, 0.5 M) and stirred vigorously. Meanwhile, to another dry round bottom flask was added **81** (483.17 mg, 2.10 mmol, 1 eq.) in dry toluene (2.63 mL, 0.8 M). The contents of the flasks were combined and stirred under argon overnight at room temperature. To quench, the solution was diluted with water and extracted with ether (x3) and brine (x1). The compound was then dried and concentrated under reduced pressure. The crude oil was purified via flash silica chromatography (5:1 ethyl acetate/hexane) affording **82** (500.0 mg, 83%) as a clear, colorless oil.

Key  $^1\text{H-NMR}$  and  $^{13}\text{C-NMR}$  Peaks for methyl (*R,E*)-5-((tert-butyl dimethylsilyl)oxy)oct-2-enoate



$^1\text{H NMR}$  (400 MHz, Chloroform-*d*):  $\delta$  6.97 (m,  $J = 15.3, 7.5$  Hz, 1H), 5.84 (d,  $J = 15.7, 1.6$  Hz, 1H), 3.83 – 3.75 (m, 1H), 3.73 (s, 3H), 2.38 – 2.27 (m, 2H), 1.45 – 1.25 (m, 5H), 0.90 (m,  $J = 7.2$  Hz, 3H), 0.88 (s,  $J = 0.7$  Hz, 9H), 0.04 (s, 6H).

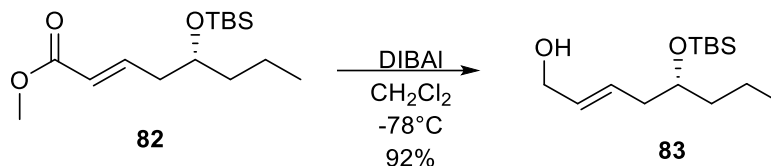
$^{13}\text{C NMR}$  (101 MHz, Chloroform-*d*):  $\delta$  146.60, 123.00, 71.28, 51.61, 40.46, 39.69, 26.05, 18.78, 14.39.

**HRMS:** calculated for  $[\text{C}_{15}\text{H}_{30}\text{O}_3\text{Si} + \text{Na}^+]$  309.1856, found 309.1860.

**Notebook:** CH2-057

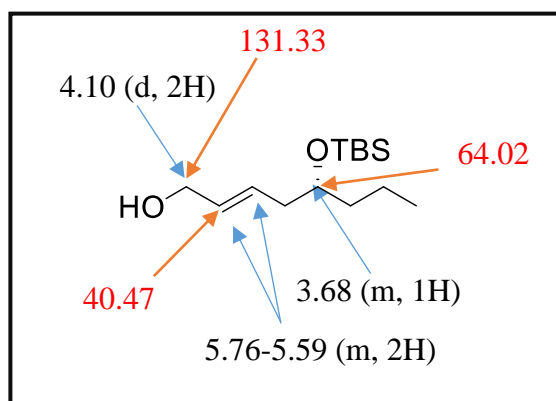


**(R,E)-5-((tert-butyldimethylsilyl)oxy)oct-2-en-1-ol**



To a flame-dried round bottom flask was added **82** (374.8 mg, 1.31 mmol, 1 eq.) and dry CH<sub>2</sub>Cl<sub>2</sub> (6.5 mL, 0.2 M). The solution was cooled to -78°C and DIBAL-H (1 M) (3.28 mL, 3.28 mmol, 2.5 eq.) was added. The solution was stirred until TLC analysis showed no remaining starting material (approximately 10-15 minutes). The solution was quenched with saturated Rochelle Salt solution and stirred overnight. The solution was extracted with CH<sub>2</sub>Cl<sub>2</sub> (x3), washed with brine (x1), dried, and concentrated. The crude oil was purified via flash silica chromatography (5:1 ethyl acetate/ hexane), affording **83** (310.96 mg, 92 %) as a clear oil.

Key <sup>1</sup>H-NMR and <sup>13</sup>C-NMR Peaks for (R,E)-5-((tert-butyldimethylsilyl)oxy)oct-2-en-1-ol

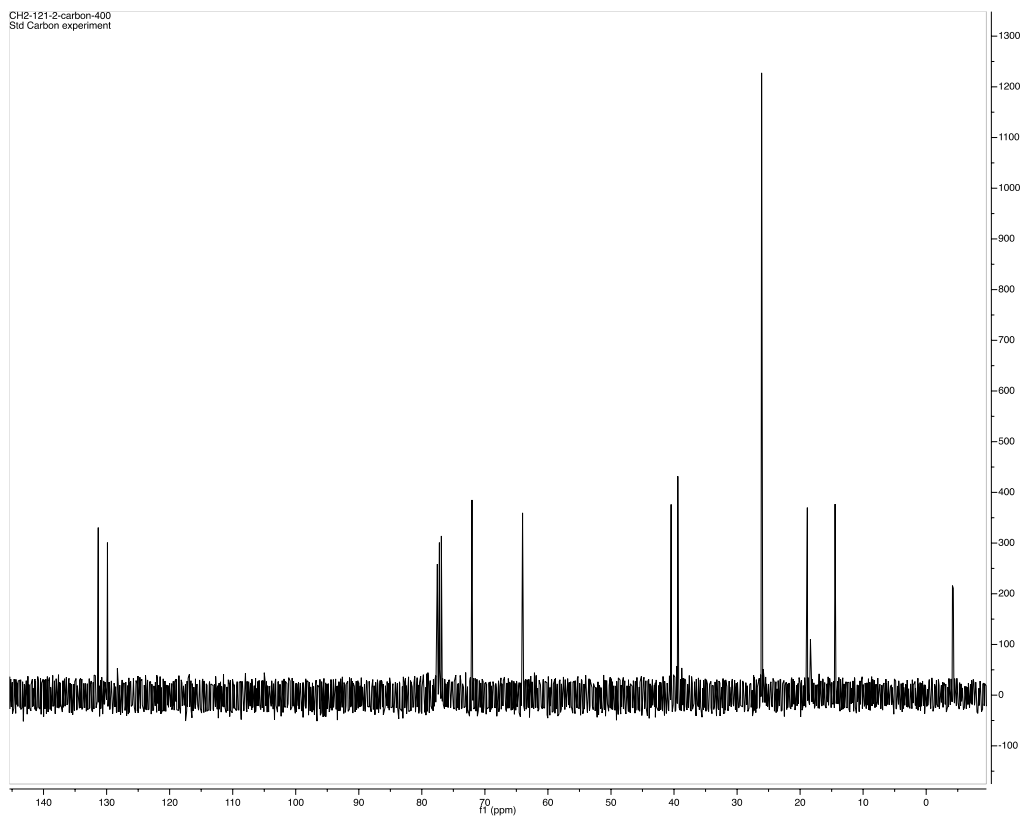
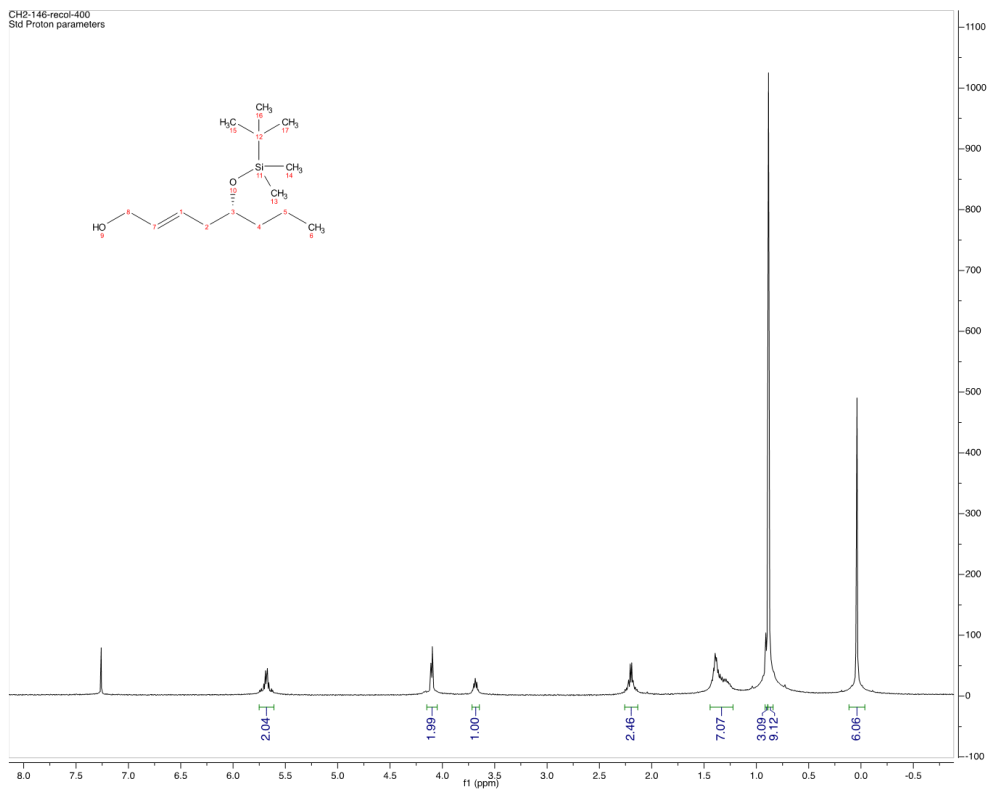


<sup>1</sup>H NMR (400 MHz, Chloroform-*d*): δ 5.76 – 5.59 (m, 2H), 4.10 (d, *J* = 4.8 Hz, 2H), 3.68 (m, *J* = 5.6 Hz, 1H), 2.20 (q, *J* = 6.0 Hz, 2H), 1.45 – 1.21 (m, 7H), 0.90 (t, *J* = 6.9 Hz, 3H), 0.88 (s, *J* = 0.9 Hz, 9H), 0.04 (s, 6H).

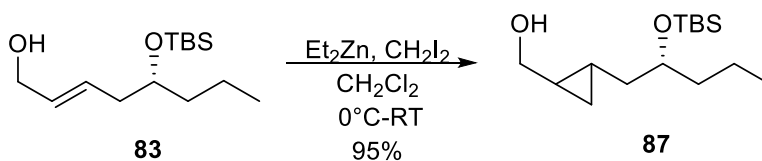
<sup>13</sup>C NMR (101 MHz, Chloroform-*d*): δ 131.33, 129.87, 72.04, 64.02, 40.47, 39.39, 26.10, 18.85, 18.37, 14.46, -4.16, -4.31.

HRMS: calculated for [C<sub>14</sub>H<sub>30</sub>O<sub>2</sub>Si + H<sup>+</sup>] 259.4845, found 259.4840.

Notebook: CH2-047

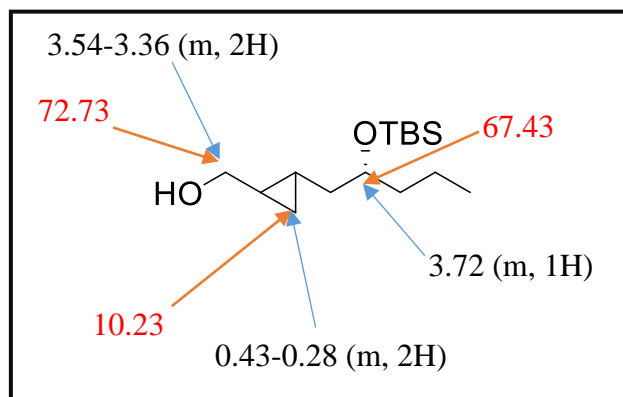


**(2-((R)-2-((tert-butyl dimethylsilyl)oxy)pentyl)cyclopropyl)methanol**



To a flame dried round bottom flask was added **83** (257.1 mg, 0.99 mmol, 1 eq.) and  $\text{CH}_2\text{Cl}_2$  (3.0 mL, 0.33 M) and was cooled to  $0^\circ\text{C}$ . To another dry round bottom flask was added diiodomethane (0.24 mL, 3.95 mmol, 2.5 eq.) and  $\text{CH}_2\text{Cl}_2$  (23 mL, 0.17 M) and was cooled to  $0^\circ\text{C}$ . To each flask was added 1 M diethyl zinc solution (1.58 mL, 1.58 mmol, 1.5 eq.). The solutions in each flask were stirred at  $0^\circ\text{C}$  for approximately 45 minutes and then combined. The remaining solution was slowly warmed to room temperature and stirred overnight under an inert atmosphere. The reaction was quenched by adding saturated ammonium chloride and 1 M HCl solution. It was then extracted with  $\text{CH}_2\text{Cl}_2$  (x3), brine (x1), dried, and concentrated under reduced pressure. The crude material was purified via flash silica chromatography (4:1 hexane/ethyl acetate) affording **87** (256.28 mg, 95 %).

Key  $^1\text{H-NMR}$  and  $^{13}\text{C-NMR}$  Peaks for  
(2-((R)-2-((tert butyldimethylsilyl)oxy)pentyl)cyclopropyl)methanol

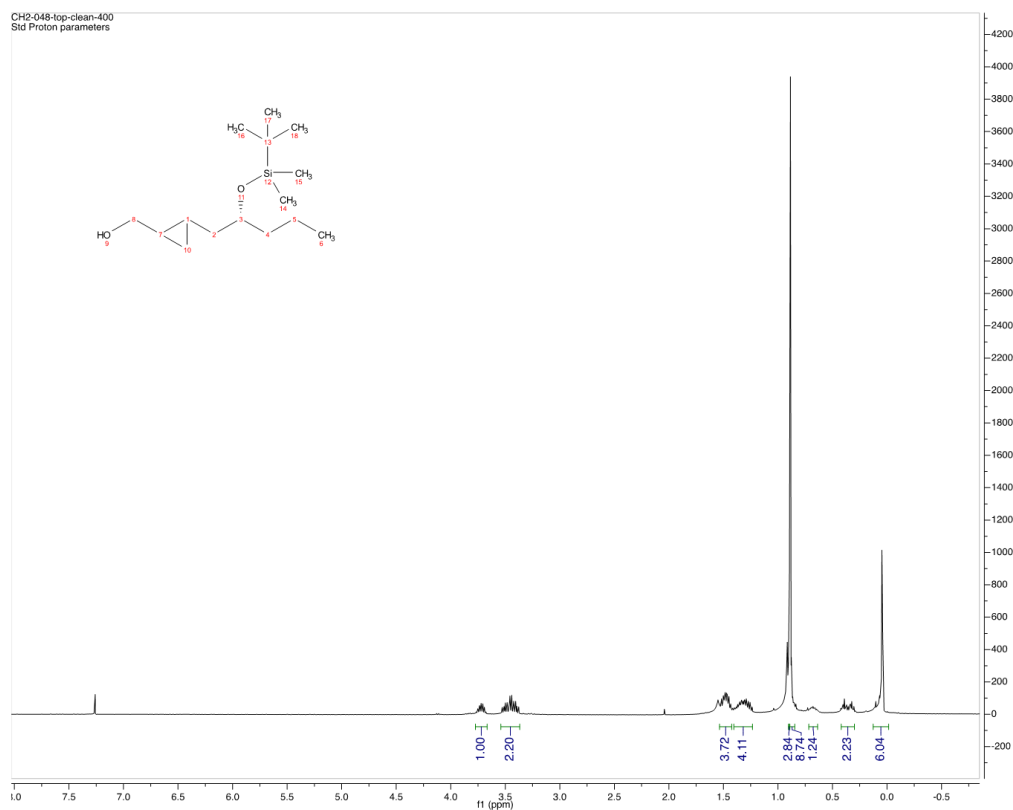


**<sup>1</sup>H NMR (400 MHz, Chloroform-*d*):** δ 3.72 (m, *J* = 11.8, 5.8 Hz, 1H), 3.54 – 3.36 (m, 2H), 1.53 (s, 1H), 1.52 – 1.43 (m, 3H), 1.39 – 1.23 (m, 3H), 0.93 – 0.89 (t, 3H), 0.89 (s, 9H), 0.73 – 0.61 (m, 1H), 0.43 – 0.28 (m, 2H), 0.05 (s, 3H), 0.04 (s, 3H).

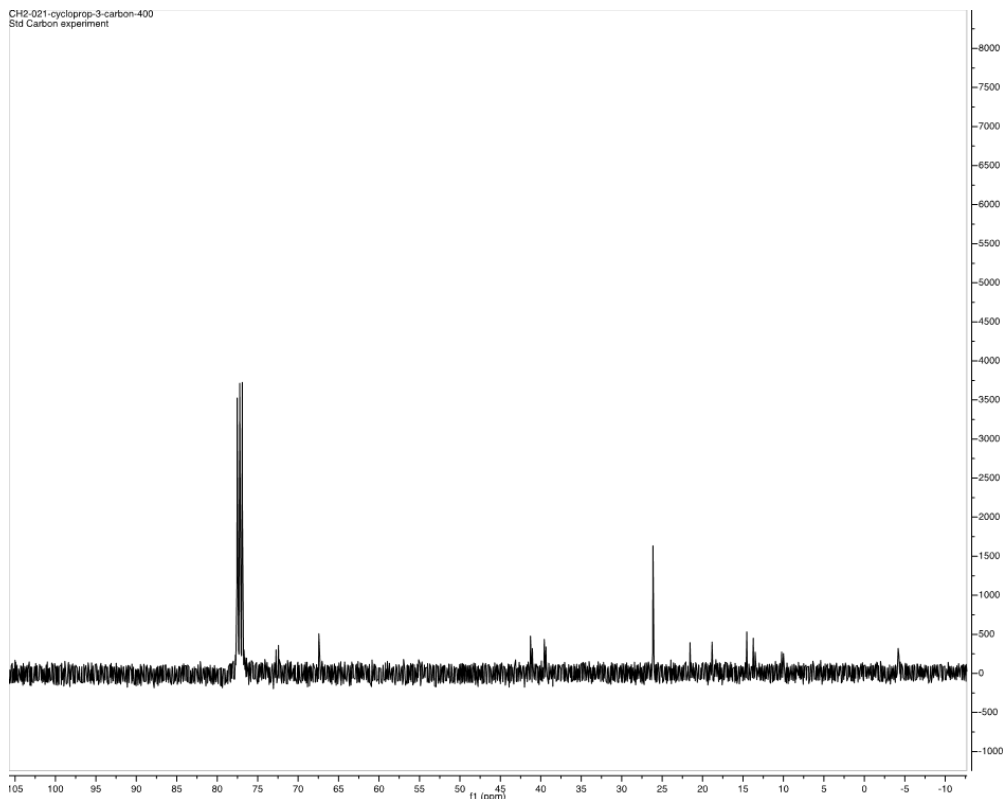
**<sup>13</sup>C NMR (101 MHz, Chloroform-*d*):** δ 72.73, 72.43, 67.43, 41.28, 41.05, 39.56, 39.35, 26.14, 21.55, 18.83, 14.54, 13.74, 13.49, 10.23, 10.00, -4.18.

**HRMS:** calculated for [C<sub>15</sub>H<sub>32</sub>O<sub>2</sub>Si + Na<sup>+</sup>] 295.4932, found 295.4934.

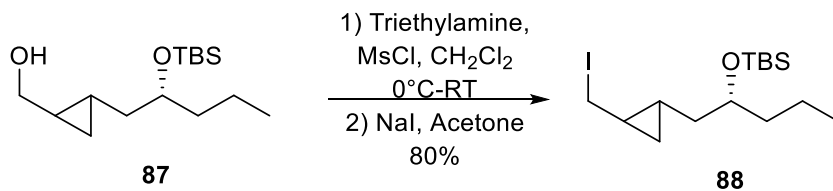
**Notebook: CH2-048**







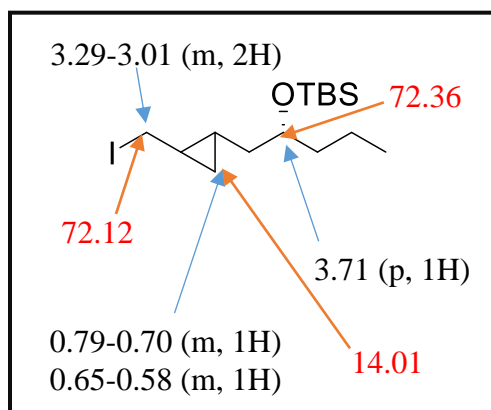
**Tert-butyl(((2R)-1-(2-(iodomethyl)cyclopropyl)pentan-2-yl)oxy)dimethylsilane**



To a dry round bottom flask was added **87** (730.0 mg, 2.68 mmol, 1 eq.), CH<sub>2</sub>Cl<sub>2</sub> (17.8 mL, 0.15 M), triethylamine (0.62 mL, 8.04 mmol, 3 eq.), and methylsulfonyl chloride (0.56 mL, 4.02 mmol, 1.5 eq.) at 0°C. The solution was stirred for approximately 10 minutes before warming to room temperature and stirring for an additional 25 minutes. The solvent was then removed under reduced pressure, resulting in a yellow solid. To the solid was added dry acetone (17.8 mL, 0.15 M) and NaI (3.62 g, 24.12 mmol, 9 eq.). The solution was stirred for 1 hour at room temperature under argon. The reaction was quenched with saturated sodium bicarbonate solution and saturated sodium thiosulfate solution, washed with ether (x3), washed with brine (x1), dried, and

concentrated under reduced pressure. The crude product was purified via flash silica chromatography (4:1 hexane/ ethyl acetate) affording **88** (910.0 mg, 80 %) as a clear oil, composed of two diastereomers.

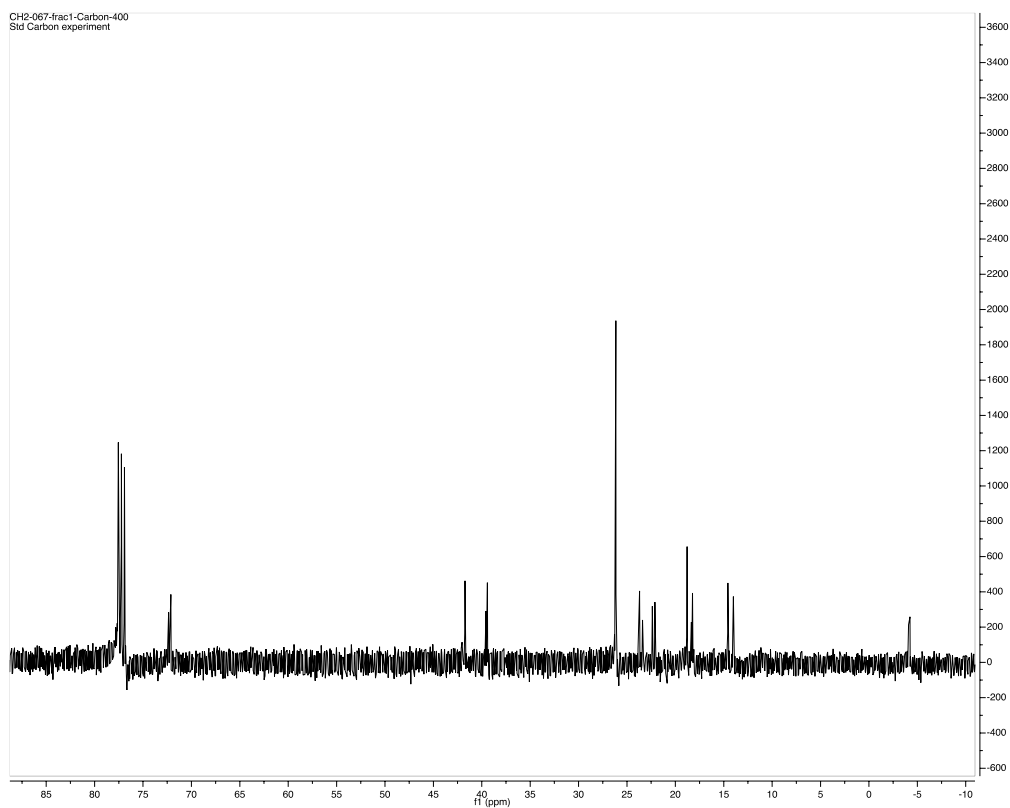
Key  $^1\text{H-NMR}$  and  $^{13}\text{C-NMR}$  Peaks of tert-butyl(((2R)-1-(2-(iodomethyl)cyclopropyl)pentan-2-yl)oxy)dimethylsilane



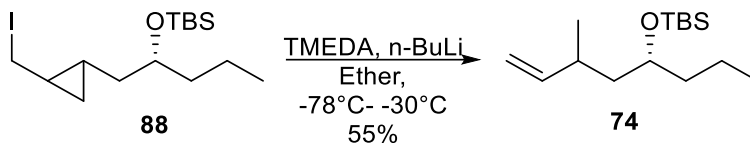
$^1\text{H NMR}$  (400 MHz, Chloroform-*d*):  $\delta$  3.71 (m,  $J = 5.7$  Hz, 1H), 3.29 – 3.01 (m, 2H), 1.56 – 1.25 (m, 8H), 1.06 (m,  $J = 8.0, 3.8$  Hz, 1H), 0.92 (t,  $J = 1.2$  Hz, 3H), 0.90 (s, 9H), 0.79 – 0.70 (m, 1H), 0.65 – 0.58 (m, 1H), 0.46 (m,  $J = 9.1, 4.7$  Hz, 1H), 0.05 (s, 3H), 0.04 (s, 3H)

$^{13}\text{C NMR}$  (101 MHz, Chloroform-*d*):  $\delta$  72.36, 72.12, 41.73, 41.68, 39.57, 39.43, 26.15, 23.70, 23.39, 22.38, 22.12, 18.79, 18.35, 18.23, 18.14, 14.58, 14.01, -4.15, -4.24.

**Notebook: CH2-142**

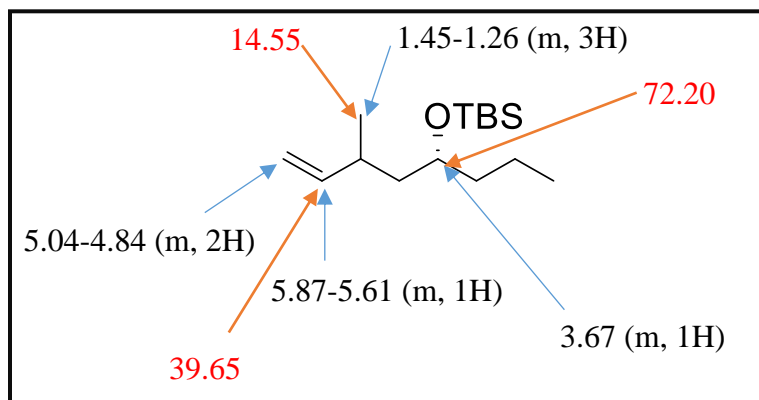


### Tert-butyldimethyl(((4R)-6-methyloct-7-en-4-yl)oxy)silane



To a dry round bottom flask was added **88** (250.3 mg, 0.65 mmol, 1 eq.), TMEDA (0.20 mL, 1.3 mmol, 2 eq.), and 1.6M n-BuLi (0.81 mL, 1.3 mmol, 2 eq.) in dry ether (3.61 mL, 0.18 M) at -78°C. After stirring for approximately 20 minutes, the solution was warmed to -30°C. The reaction was quenched with water after stirring for approximately 3.5 hours. It was then extracted with ether (x3), 10% HCl (x1), saturated sodium carbonate (x1), and brine (x1), dried, and concentrated under reduced pressure. The crude product was purified via flash silica chromatography (10:1 hexane/CH<sub>2</sub>Cl<sub>2</sub>) producing **74** (166 mg, 55%).

Key <sup>1</sup>H-NMR and <sup>13</sup>C-NMR Peaks for tert-butyldimethyl(((4R)-6-methyloct-7-en-4-yl)oxy)silane



**<sup>1</sup>H NMR (400 MHz, Chloroform-*d*):** δ 5.86 – 5.63 (m, 1H), 5.04 – 4.87 (m, 2H), 3.67 (m, *J* = 15.0, 10.1, 5.5 Hz, 1H), 2.24 (m, *J* = 14.3, 7.2 Hz, 1H), 2.03 (m, *J* = 6.9 Hz, 1H), 1.48 – 1.30 (m, 3H), 0.98 (d, *J* = 6.7, 2.8 Hz, 3H), 0.90 (t, *J* = 3.6 Hz, 3H), 0.88 (s, *J* = 0.8 Hz, 9H), 0.04 (s, 6H).

**<sup>13</sup>C NMR (101 MHz, Chloroform-*d*):** δ 139.23, 114.50, 112.50, 112.46, 72.20, 44.47, 39.65 (d, *J* = 7.2 Hz), 34.47, 24.80, 20.52, 18.47, 14.55, -4.06.

**HRMS:** calculated for [C<sub>15</sub>H<sub>32</sub>OSi + Na<sup>+</sup>] 279.4942, found 279.4939.

**Notebook:** CH2-082



## Chapter 6: Bibliography

1. Ball, P. Chemistry: Why synthesize? *Nature* **2015**, 528, 327-329
2. Wu, A. Chinese Tea. [www.chinahighlights.com/travelguide/chinese-tea](http://www.chinahighlights.com/travelguide/chinese-tea).
3. Root, J. 40 Amazing Uses for Aloe Vera.  
<http://health.howstuffworks.com/wellness/natural-medicine/herbal-remedies/amazing-aloe-vera.htm> .
4. WebMD. Vitamins and Supplements: Coca. <http://www.webmd.com/vitamins-supplements/ingredientmono-748-coca.aspx?activeingredientid=748&> .
5. Edgar, J. Medicinal Uses of Honey.<http://www.webmd.com/diet/features/medicinal-uses-of-honey#1> .
6. Demain, A.; Fang, A. Natural function of secondary metabolites. *Advances in Biochemical Engineering/ Technology* **2000**, 69.
7. Wilkins, S.P; et al. Isolation of an antifreeze peptide from the Antarctic sponge *Homaxinella balfourensis*. *Cellular Molecular Life Sciences* **2002**, 59, 2210-2215.
8. Erbguth, F. From poison to remedy: the chequered history of botulinum toxin. *Journal of Neural Transmission* **2008**, 559-565.
9. Nigam, P.; Nigam, A. Botulinum Toxin. *Indian Journal of Dermatology*. **2010**, 8-14.
10. Lindstrom, M.; H. Korkeala, H. Laboratory diagnostics of botulinum. *Clinical Microbiology Reviews*. **2006**, 19, 298-314
11. Lacy, D. B.; Tepp, W.; Cohen, A. C.; DasGupta, B.R.; Stevens, R. C. Crystal Structure Of Botulinum Neurotoxin Serotype A. *Nature Structural & Molecular Biology* **1998**, 898-902.
12. Connelly, D. A history of aspirin. *The Pharmaceutical Journal: A Royal Pharmaceutical Society Publication* **2014**.
13. Lewis, D. Aspirin: A curriculum resource for post-16 chemistry and science courses. *Royal Society of Chemistry* **1998**, 1-32.
14. Goldberg, D. R. Aspirin: Turn of the Century Miracle Drug. *Chemical Heritage Foundation* **2009**.

15. Liebmann, J.E.; Cook, J.A.; Lipschultz, C.; Teague, J. F.; Mitchell, J.B. Cytotoxic studies of paclitaxel (Taxol) in human tumour cell lines. *British Journal of Cancer* **1993**, 1104-1109.
16. Nicolau, K.C; Nantermet, P.G.; Ueno, H.; Guy, R. K.; Couladuoros, E. A.; Sorenson, E. J. Total Synthesis of Taxol. 1. Retrosynthesis, Degradation, Reconstitution. *Journal of the American Chemical Society*, **1995**, 117 (2), 624-633.
17. Borman, S. Scientists Mobilize To Increase Supply of Anticancer Drug, Taxol. *Chemical & Engineering News* **1991**, 11-18.
18. Weaver, B. How Taxol/paclitaxel kills cancer cells. *Molecular biology of the cell* **2014**, 2677-2681.
19. Chooljian, S. H.; Kauffman, G. B. Wohler's synthesis of artificial urea: A modern version of a classic experiment. *Journal of Chemical Education* **1979**, 197.
20. Nicolau, K. C. Organic synthesis: the art and science of replicating the molecules of living nature and creating others like them in the laboratory. *Proceedings of the Royal Society* **2013**.
21. Siegel, R.; Miller, K.; Jemal, A. Cancer Statistics, 2017. *CA: A Cancer Journal for Clinicians* **2017**, 7-30.
22. Lebar, M.; Heimbegner, J.; Baker, B. Cold-water marine natural products. *Natural Products Reports* **2006**, 34, 585-626.
23. Falkenberg, M. ; Rangel, M. An overview of the marine natural products in clinical trials and on the market. *Journal of Coastal Life Medicine* **2015**, 3(6): 421-428.
24. Suenaga, K.; Mutou, T.; Shibata, T.; et al. Aurilide, a cytotoxic depsipeptide from the sea hare *Dolabella auricularia*: isolation, structure determination, synthesis, and biological activity. *Tetrahedron* **2004**, 8509-8527.
25. Tripathi, A.; Puddick, J.; Lebel, H.; et al. Lagunamide C, a cytotoxic cyclodepsipeptide from the marine cyanobacterium *Lyngbya majuscula*. *Phytochemistry* **2011**, 2369-2375.
26. Tan, L. T.; Gupta, D. K. Aurilides/Lagunamides. *Handbook of Anticancer Drugs from Marine Origin*; Kim, S.-K., Ed.; Springer, **2015**, 580-581.
27. Dai, L.; Chen, B; Lei, H.; et al. Total synthesis and stereochemical revision of lagunamide A. *Chemical Communications* **2012**, 8697-8699.

28. Pal, S.; Chakraborty, T. Toward the total synthesis of a lagunamide B analogue. *Tetrahedron Letters* **2014**, 3469-3472.
29. Tripathi, A.; Puddick, J.; Prinsep, M.; et al. Lagunamides A and B: Cytotoxic and Antimalarial Cyclodepsipeptides from the Marine Cyanobacterium *Lyngbya majuscula*. *Journal of Natural Products* **2010**, 1810-1814.
30. Crimmins, M. T.; King, B. W.; Tabet, E. A.; Chaudhary, K. Asymmetric Aldol Additions: Use of Titanium Tetrachloride and (-)-Sparteine for the soft enolization of N-Acyl Oxazolidinones, Oxazolidinethiones, and thiazolidinethiones. *Journal of Organic Chemistry* **2001**, 66 (3), 894–902.
31. Hodge, M.; Olivio, H. Stereoselective aldol additions of titanium enolates of N-acetyl-4-siopropyl-thiazolidinethione. *Tetrahedron* **2004**, 9397-9403.
32. Charette, A.; Juteau, H.; *et.al.* Enantioselective cyclopropanation of allylic alcohols with dioxaborolane ligands: Scope and synthetic applications. *Journal of American Chemical Society* **1998**, 11943-11952.
33. Mohapatra, D. K.; Nayak, S. Stereoselective synthesis of the C33-C44 fragment of palauamide. *Tetrahedron Letters* **2008**, 49, 786-789.
34. Lister, T.; Perkins, M. A retro-Claisen approach to dolabriferol. *Organic Letters* **2006**, 8 (9), 1827–1830.
35. Sinz, C. J.; Rychnovsky, S. D. Total synthesis of the polyene macrolide dermostatin A. *Tetrahedron* **2002**, 58: 6561-6576.
36. Corey, E. J.; Helal, C. J. Reduction of Carbonyl Compounds with Chiral Oxazaborlidine Catalysts: A New Paradigm for Enantioselective Catalysis and a Powerful New Synthetic Method. *Angewante Chemie International Edition* **1998**, 37, 1986–2012.
37. Zhou, H.; Gao, Z.; Qiao, K.; Wang, J.; Vederas, J. C.; Tang, Y. A fungal ketoreductase domain that displays substrate-dependent stereospecificity. *Nature Chemical Biology* **2012**, 8, 331-333.